



HHS Public Access

Author manuscript

Biochim Biophys Acta Biomembr. Author manuscript; available in PMC 2022 September 01.

Published in final edited form as:

Biochim Biophys Acta Biomembr. 2021 September 01; 1863(9): 183643. doi:10.1016/j.bbamem.2021.183643.

Exploring lipid-dependent conformations of membrane-bound α -synuclein with the VDAC nanopore

David P. Hoogerheide¹, Tatiana K. Rostovtseva^{2,*}, Sergey M. Bezrukov²

¹Center for Neutron Research, National Institute of Standards and Technology, Gaithersburg, MD 20899, USA

²Section on Molecular Transport, Eunice Kennedy Shriver National Institute of Child Health and Human Development, National Institutes of Health, Bethesda, MD 20892, USA.

Abstract

Regulation of VDAC by α -Synuclein (α Syn) is a rich and instructive example of protein-protein interactions catalyzed by a lipid membrane surface. α Syn, a peripheral membrane protein involved in Parkinson's disease pathology, is known to bind to membranes in a transient manner. α Syn's negatively charged C-terminal domain is then available to be electromechanically trapped by the VDAC β -barrel, a process that is observed *in vitro* as the reversible reduction of ion flow through a single voltage-biased VDAC nanopore. Binding of α Syn to the lipid bilayer is a prerequisite of the channel-protein interaction; surprisingly, however, we find that the strength of α Syn binding to the membrane does not correlate in any simple way with its efficiency of blocking VDAC, suggesting that the lipid-dependent conformations of the membrane-bound α Syn control the interaction. Quantitative models of the free energy landscape governing the capture and release processes allow us to discriminate between several α Syn (sub-) conformations on the membrane surface. These results, combined with known structural features of α Syn on anionic lipid membranes, point to a model in which the lipid composition determines the fraction of α Syn molecules for which the charged C terminal domain is constrained to be close, but not tightly bound, to the membrane surface and thus readily captured by VDAC nanopore. We speculate that changes in the mitochondrial membrane lipid composition may be key regulators of the α Syn-VDAC interaction and consequently of VDAC-facilitated transport of ions and metabolites in and out of mitochondria and, therefore, mitochondrial metabolism.

Graphical Abstract

* To whom correspondence should be addressed: Tatiana K. Rostovtseva, Section on Molecular Transport, Eunice Kennedy Shriver National Institute of Child Health and Human Development, National Institutes of Health, 9000 Rockville Pike, Bldg. 29B, Room 1G09, Bethesda, MD 20892-0924. Phone: (301) 402-4702, rostovtt@mail.nih.gov.

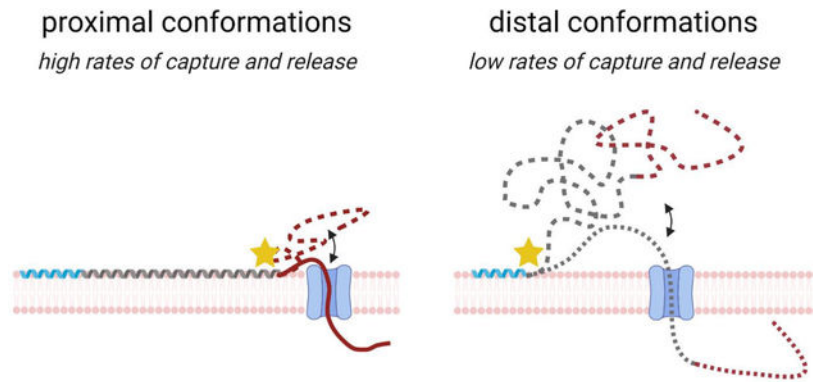
Conflict of Interests

The authors declare that they have no competing interests with the contents of this article.

Declaration of competing interests

The authors declare that they have no known competing financial interests or personal relationships that could have appeared to influence the work reported in this paper.

Publisher's Disclaimer: This is a PDF file of an unedited manuscript that has been accepted for publication. As a service to our customers we are providing this early version of the manuscript. The manuscript will undergo copyediting, typesetting, and review of the resulting proof before it is published in its final form. Please note that during the production process errors may be discovered which could affect the content, and all legal disclaimers that apply to the journal pertain.



Keywords

voltage-dependent anion channel; protein-lipid interaction; single-molecule measurement; energy landscape; mitochondrial lipids; a-hemolysin

1. Introduction

The voltage-dependent anion channel (VDAC) is the most abundant protein at the mitochondrial outer membrane (MOM). Oxidative phosphorylation—the main function of mitochondria—requires efficient exchange of respiratory substrates, such as ATP, ADP, pyruvate, succinate, and inorganic phosphate, between mitochondria and the cytosol. The large share of the MOM's permeation functions is executed by VDAC, which conducts and regulates fluxes of water-soluble metabolites and small ions in and out of mitochondria. It is VDAC's unique location at the interface between mitochondria and the cytosol that ensures its central role in bioenergetics and cell metabolism by enabling its interaction with cytosolic proteins involved in multiple signaling and metabolic pathways [1, 2]. Indeed, VDAC was found associated with a plethora of different pro-survival and pro-apoptotic proteins, endogenous and synthetic steroids, and anti-cancer and neuroprotective drugs (for review see e.g., [3–5]) and was consequently reported to be implicated in various diseases from cancer to neurodegeneration [6, 7].

Despite its impressive multifunctionality, VDAC is relatively uncomplicated. It is a monomeric channel comprising 19 β -strands that define a 2.7 nm diameter pore. A broken α -helix that lies along one side of the channel wall, approximately equidistant from the two ends of the pore, reinforces the β -barrel [8] and creates a constriction zone of about 1.4 nm in the narrowest part [9–11] (Figure 1). There is some evidence that this N-terminal α -helix takes part in the gating process [12–15]. VDAC is a passive diffusion channel that allows the passage of non-charged polymers up to 2 – 5 kDa [16, 17] and disordered polypeptide chains [18]. When reconstituted into planar lipid membranes—so far the only available method to study this channel's biophysical properties—VDAC forms large, weakly anion-selective channels with a conductivity of about 4 nS in 1 M KCl ($M = \text{mol/L}$). In 150 mM KCl, the conductance is about 0.7 nS [19] and the permeability ratio $\text{Cl}^-/\text{K}^+ \sim 3$ [16, 20, 21]. VDAC's anion selectivity matches the negative charge of most mitochondrial metabolites, such as ATP and ADP.

VDAC's name derives from its characteristic voltage gating behavior. Unlike VDAC's structure, voltage gating is complicated, and, despite being known since 1976 when this mitochondrial channel was biophysically characterized first by Marco Colombini [22–24] and then by others [25–29], is still not explained by a quantitative and comprehensive model (see, e.g. discussion in [30–32]). Gating, by definition, is VDAC's ability to stochastically transition under transmembrane potentials of > 30 mV from a unique anion-selective high-conducting “open” state to a variety of less anion-selective, low-conducting “closed” states. Importantly, the open state is open for ATP transport and the closed states are essentially impermeable to ATP [33, 34], mostly due to the reduced anion selectivity of the closed states. The closed states still conduct small ions and appear to be significantly more permeable for calcium ions than for chloride ions [35]. These distinctive biophysical properties of VDAC's different states suggest that by gating VDAC could regulate fluxes of metabolites and calcium *in vivo* [36]. Its open state facilitates ADP uptake and keeps calcium influx low, thus maintaining normal respiration, while its closed states reduce metabolite transport but increase calcium uptake leading to respiration impairment. Therefore, VDAC gating, though observed so far only on reconstituted channels, is likely to be one of the mechanisms that control MOM permeability in cells [1, 33, 35–38]. The sensitivity of VDAC gating to the lipid environment is particularly intriguing [39–41] but remains poorly understood. Progress in computational methods and high-resolution spectroscopy may provide additional insight in the near future. Regardless, VDAC gating as a mechanism to control mitochondrial metabolism *in vivo* meets a serious obstacle: the uncertainty concerning the real value of the membrane potential across MOM (e.g., see discussions in [1, 37, 42]).

Considering all the above, the search for VDAC regulation then expands to include its interactions with cytosolic proteins. Of these, dimeric tubulin and alpha-synuclein (α Syn) have emerged as potent VDAC regulators [18, 43–47] due to their cytosolic abundance and the efficiency of their interactions with VDAC *in vitro* and *in vivo*. Here we focus on α Syn and discuss the possible mechanisms by which mitochondria may tune the efficiency of such regulation.

α Syn is an intrinsically disordered neuronal protein and a well-known pathological hallmark of Parkinson's disease (PD) [48]. It was initially found in the fibrillar form in the so-called Lewy bodies of the post-mortem brains of PD patients [49]. In normal neurons, α Syn constitutes up to 1 % of the total cytosolic protein content [50] and exists mainly as monomers, not as the fibrillar form associated with pathology (Fig. 2A). While fibrillar forms of α Syn are undoubtedly linked to PD or other synucleinopathies, the physiological role of its monomeric form remains poorly understood. In mitochondria, α Syn in oligomeric and monomeric forms is found in association with both the inner and outer membranes [45, 51–53], causing typical mitochondrial dysfunctions, such as oxidative stress [54], impairment of the respiratory complexes [53, 55–57], or fission [58]. All these studies showed that when the α Syn expression level in a cell increases, α Syn enters the mitochondria and targets respiratory complexes at the mitochondrial inner membrane (MIM), inducing mitochondrial dysfunction. However, the molecular identity of the pathway for α Syn to cross the MOM has long been a mystery. Initially, Tom40, the channel component of the translocase of the outer membrane (TOM complex), was suggested as a

possible candidate for such pathway [56]. Later, our group unambiguously proved that VDAC is indeed a gateway for α Syn entry into mitochondria. Using electrophysiological single-channel experiments with VDAC reconstituted into planar lipid membranes, we showed that α Syn effectively and reversibly blocks the VDAC pore at nanomolar concentrations; under some conditions, determined by the applied potential, lipid composition, or ionic strength of membrane-bathing solution, α Syn translocates through VDAC [18, 59, 60]. These results will be detailed throughout this review. By contrast, α Syn does not measurably affect the conductance of Tom40 reconstituted into planar membranes [61]. Further, using neuronally differentiated human cells overexpressing wild-type α Syn as an adequate cell model of PD, we showed that α Syn translocates into mitochondria, causing the loss of mitochondrial potential and consequent cell death, and that the VDAC1 isoform is required for α Syn translocation [45].

The immediate question is what are the endogenous factors that regulate the discovered α Syn-VDAC interaction *in vivo*? One would expect that the α Syn expression level [45, 56], its disease-related mutations [62], post-translational modifications (PTM) [63, 64], and different cytosolic factors such as pH [65] could affect this process. Here we address the question of how α Syn-VDAC interaction could be regulated by mitochondria. Leaving aside the role of transmembrane voltage briefly discussed above, we focus instead on the less obvious but no less important role of mitochondrial lipids in α Syn-VDAC interaction. We will show that mitochondria lipids turn out to be one of the tools for mitochondria to fulfill this task.

Mitochondrial lipids of both outer and inner membranes play important structural and functional roles in maintaining mitochondrial biogenesis. Changes in the phospholipid composition affect mitochondrial functions and dynamics and have been linked to a variety of human diseases such as Barth syndrome [66], heart failure [67], neurodegenerative diseases [68], and cancer [69]. Considering the substantial lipid homeostasis in mitochondria during morphological changes such as fusion and fission [70], interorganellar interaction through mitochondria-associated membranes [71], apoptotic stress [72], or lipid oxidation by the reactive oxygen species produced by mitochondria [73–75], lipids could be potent regulators of α Syn-VDAC interaction, thus controlling VDAC permeability *in vivo*.

In this review, we will show that single-molecule electrophysiology, using VDAC reconstituted into lipid bilayer membranes mimicking the mammalian MOM composition, reveals a strong dependence of the *in vitro* interaction of VDAC with α Syn on the detailed chemical composition of the lipid bilayer. We complement known structural properties of α Syn on lipid membranes with single-molecule interrogation using nanopores; this combination allows us to identify structural details of the distributions of conformations adopted by α Syn on lipid surfaces.

Throughout the discussion, VDAC will play a dual role. VDAC is a mitochondrial channel, a tunable transporter of polyvalent metabolites; as such, a target for α Syn. VDAC is also a nanopore, a passive ionic conductor, a source of electromechanical force, and a reporter on the presence and charge composition of polypeptide chains it is able to capture; as such, VDAC will be a probe for the α Syn presence and conformation at the lipid membrane. It is

our contention that at the intersection of these dual roles—target vs. nanoprobe sensor—we gain the most insight into the biophysical chemistry of the α Syn-VDAC interaction, as catalyzed by the membrane surface. In other words, the use of VDAC, the very mitochondrial protein targeted by α Syn, as a nanopore probe provides unique mechanistic details of their interaction.

In Section 2, we will first briefly discuss the structure of α Syn on membrane surfaces and the role of lipid composition. Section 3 will introduce the principles of using a membrane-embedded nanopore as a local single-molecule probe for α Syn. Section 4 will detail the observations regarding the role of lipids in the interaction of α Syn with VDAC. Section 5 will relate these findings to the structural data reviewed in Section 2. Immediate physiological implications of the α Syn-VDAC interaction will be discussed in Section 6. Using a different, asymmetric nanopore of α -hemolysin, in Section 7 we will show that the nanopore-captured α Syn molecules are predominantly bound to membrane surfaces and then discuss the differences between the results obtained with this more traditional protein nanopore and VDAC.

2. Structure of membrane-bound α Syn

The structure of α Syn on lipid membranes is of significant contemporary interest, primarily due to the interplay between α Syn lipid membrane binding and its aggregate formation [76–80]. α Syn is disordered in solution but does have three distinct regions that respond differently to membrane surfaces and other α Syn molecules (Figure 2A) [81–84]. The amphipathic region is the membrane-binding domain, whereas the central nonpolar or so called NAC (non-amyloid b component) domain is involved in fibril formation [85]. While the first two regions obtain structural features, the polyanionic C-terminal tail (CTT) remains disordered.

Early NMR studies showed [86] that the membrane-binding region of α Syn adopts a broken amphipathic helical conformation when associated with anionic SDS micelles. There were also early hints pointing to conformational variability, as small populations that deviated from the majority conformation were also observed. Later NMR results [81] obtained with anionic small unilamellar vesicles also identified an extended amphipathic binding motif in the α Syn N-terminal domain (Figure 2B). The binding domain comprises two helical regions, one of which remains consistently membrane-associated. The other spans part of both the amphipathic and NAC domains and is thought to be in dynamic equilibrium between the helical, membrane-associated (“proximal”) and disordered, membrane-dissociated (“distal”) states (Figure 2B) [81]. In crosslinked mutants, the membrane binding energy differences among various conformers of α Syn on anionic lipid surfaces were shown to be minimal, suggesting that a variety of binding conformations are likely to be populated even on anionic surfaces [87].

Neutron reflectivity data with segmentally deuterated α Syn confirmed that on anionic lipid surfaces the membrane-binding region of α Syn resides at the interface between the lipid acyl chains and the headgroups, while the CTT is found above the lipid membrane (Figure 2C) [88, 89]. Complementary Trp fluorescence results showed that, when associated with these

lipid surfaces, residue 94 appears to be held deeply buried into the lipid acyl chains [90], consistent with the results of Fusco et al. [81] for the membrane-associated state of the entire N-terminal domain.

The structure of α Syn on uncharged or weakly charged membranes is less extensively characterized. Circular dichroism reveals that α Syn remains unstructured in the presence of phosphatidylcholine (PC) vesicles [79]. α Syn does bind to PC lipids, however; high concentrations of α Syn can also cause tubulation of PC membranes [79], while binding is observed by Fluorescent Correlation Spectroscopy (FCS) and isothermal titration calorimetry [87, 91, 92].

3. Nanopore probes for surface-bound proteins

The use of nanopores—single perforations in a thin membrane that physically and electrically isolates two electrolyte-filled reservoirs—for single-molecule or single-particle analysis now has several decades of history. The principle is the same as that of a Coulter counter [93, 94]: the time-dependent modulation in ion transport through a voltage-biased nanopore, as revealed by the measured ionic current, reports on the dynamics of the internal state of the channel. Nanopores are effective in a number of applications, including measurement of chemical kinetics [95, 96], nucleic acid sequencing [97, 98], and more recently for protein sequencing [99], sensing of protein-protein interactions [100], detection of post-translational modifications [101], protein translocation [102, 103], and quantification of protein-lipid binding conformation and energetics [104].

In principle any channel is suitable as a nanopore, provided its internal dynamics can be separated from those that are caused by its interactions with analytes [105]. VDAC is one such channel; while its name derives from its characteristic gating response to voltage, under appropriate experimental conditions such as lipid composition [19, 25, 106], ionic strength [19, 25], or pH [107, 108], VDAC spends most of its time as a quiescent, passive transport channel.

Figure 3A shows a schematic of the sensing process of α Syn with a generic nanopore. Under an applied transmembrane potential, an ionic current is set up through the nanopore. When a charged polyelectrolyte, such as a nucleic acid or polypeptide, diffuses near the pore opening, it can be captured in the electric field and inserts into the channel. This process causes a modulation (reduction or increase, depending on the details of the bathing electrolyte and the captured molecule itself [109, 110]) of the ionic current through the nanopore (Figure 3B). After some time, the captured molecule leaves the nanopore, and the ionic current is restored to its original, analyte-free value. The entire process, known colloquially as an “event”, encodes information about the interaction of a single polyelectrolyte with a single pore. The event-specific observables are (1) the time elapsed before the event t_{on} , (2) the duration t_{off} and, with sufficiently low noise at the required time resolution, (3) the time-dependent details of the ionic current modulation, $I(t)$, during the event. When many events are observed for the same nominal analyte-nanopore interaction, additional observables unique to single-molecule detection are in play, including detailed statistical analysis of the events and their correlations in time. Two of these multi-event

observables are the mean time between events, $\tau_{on} = \langle t_{on} \rangle$, and the average event duration, $\tau_{off} = \langle t_{off} \rangle$, where the brackets denote averages.

In single-channel experiments with VDAC reconstituted into a planar bilayer, nanomolar concentrations of α Syn added to either side of the bilayer induce characteristic blockage events, detectable only when a negative potential is applied to the side of addition [18] (Figure 4A). This observation and the fact that the rate of blockage events by modified α Syn with a half-truncated C-terminal domain is reduced by orders of magnitude in comparison with the wild-type, allowed us to suggest that the polyanionic 45-residue CTT of α Syn is the VDAC pore blocking domain [18].

The results obtained with α Syn-VDAC interactions have led to a 3-step model (Figure 3C). In the first step, α Syn binds to the lipid membrane by its N-terminal domain [111]. In the second step, the polyanionic C-terminal domain, driven by the negative potential, is captured in the pore; the continued motion of α Syn is arrested by the N-terminal anchor and the α Syn molecule is electromechanically trapped. The third step is release of the C-terminal domain from the pore, either by the thermal motion-driven retraction from the nanopore or translocation of the whole α Syn molecule through the pore following unbinding of the N-terminal anchor from the membrane [18, 47]. The retraction process is characterized by an exponential *increase* of blockage time with voltage [18] (Figure 3D). Above a critical voltage—the “turnover” potential V^* —the blockage time *decreases* with voltage. Direct measurements of the translocation probability (Figure 5) show that in this regime nearly all α Syn molecules translocate [18, 60].

Figure 5 demonstrates that the processes depicted in Figure 3C can be quantitatively described by a free energy profile of the reaction [112]. An example of a free energy profile is shown in Figure 3E. The following subsections will discuss the two regions of the free energy profile governing capture (dashed lines on the lefts in Figure 3E) and release (solid line), and what can be learned from experimental observations of each. It is important to note that the essential features of the VDAC- α Syn interaction, such as the voltage-dependence of blockage durations and probability of α Syn translocation, can be described by a free energy profile incorporating the physical properties of the α Syn molecule, rather than those of VDAC [60, 101]. This constitutes conclusive evidence that the observed interaction mechanism is voltage-induced insertion of α Syn into the VDAC nanopore, rather than α Syn-induced gating of the VDAC channel.

3.1. Capture kinetics (the “on-rate”)

The rate of capture of molecules into a nanopore, $k_{on} = \tau_{on}^{-1}$, reveals important information about the underlying physical interaction. Indeed, in a diffusion-limited case, the nanopore captures with almost total efficiency each molecule that arrives in its vicinity. In this case one expects a weak dependence on the transmembrane potential. In a barrier-limited case, in which capture is inefficient due to the presence of an energetic barrier (*e.g.* the entropic cost of confinement), the capture rate is likely to depend exponentially on the applied transmembrane potential [113]. This is the regime that applies to the VDAC- α Syn

interaction (Figure 3D, blue line). Using a Kramers-type formalism [114], the capture rate can be written:

$$k_{on} = \omega \exp(-\Delta G_{on}^{\ddagger}) \quad (1)$$

Here, ω is a collision rate between α Syn and the nanopore that is usually proportional to the relevant concentration (surface or solution), and the exponential factor represents a success rate based on the height of the energy barrier to pore entry by the molecule. This energy barrier height has multiple contributions, e.g.

$$\Delta G_{on}^{\ddagger} = q_{on} V + \Delta G_{confinement} + \Delta G_{conformation} + \dots \quad (2)$$

Here the first term represents the effect of the fraction of the transmembrane potential that extends beyond the nanopore into the bulk and can be characterized by an effective charge q_{on} of the molecule; $G_{confinement}$ is the entropic cost to confine the molecule in the pore; and $\Delta G_{conformation}$ represents any energy required to rearrange the molecular conformation before capture by the pore. This region of the free energy profile, shown as a dashed line on the left in Figure 3E, can be directly probed with a nanopore only in very special circumstances [115], because in general the nanopore does not interrogate the α Syn molecule until it is already captured in the nanopore.

In sum, a panoply of effects can influence k_{on} . The mentioned contributions to the exponent argument (Eq. 2) have the largest impact, though k_{on} is also proportional to the concentration of the analyte. Note that the capture can occur either from solution (as is typically the case for nucleic acids), or from the surface of the membrane. In Section 7 of this review, we will show that α -hemolysin—a different, pronouncedly asymmetric β -barrel nanopore—reveals that more than 99.9 % of the α Syn molecules captured by the membrane-embedded nanopores are bound to the lipid surface. We will also see that the profound lipid dependence of the free energy profile further supports this conclusion and demonstrates that k_{on} is sensitive not only to the total amount of membrane-bound α Syn, but also to the conformations α Syn adopts on the membrane surface.

3.2. Release kinetics (the “off-rate”)

Compared to the on-rate, the physics of the off-rate distribution of a polyelectrolyte has a more quantifiable theoretical basis and can be directly interrogated by the VDAC nanopore. The theory relies on the key insight that the forces acting on the polyelectrolyte can be expressed as the gradient of a one-dimensional potential function $U(x)$, where the spatial dimension x is the linear progress of the polyelectrolyte through the nanopore. Thus, each boundary of the interval x corresponds to one or the other end of the linear polyelectrolyte chain in the nanopore (Figure 3E). The three-dimensional variability in the conformations explored by the captured polyelectrolytes can also be expressed as a one-dimensional entropic free energy [116].

An example of $U(x)$ is shown as the solid line in Figure 3E. The local free energy minimum, labeled (1), is formed by two major free energy terms: the electrostatic interaction with the transmembrane potential, and the binding energy to the membrane. In the Kramers picture, the former is primarily responsible for the free energy barrier to retraction, ΔG_{ret}^\ddagger , while the latter is primarily responsible for the free energy barrier to translocation, $\Delta G_{trans}^\ddagger$. Put simply, to retract the charged CT domain, α Syn must work against the electrodynamic forces that captured it; while to translocate, the α Syn molecule must unbind from the lipid membrane surface. The difference in these two free energies determines the partitioning of the population of the captured α Syn molecules between retraction and translocation, and hence the translocation probability P_{trans} .

Because $U(x)$ can be written as the sum of physically relevant terms, however, we do not have to rely on a Kramers-like description. $U(x)$ is directly related to the measured distribution of off-rates via the adjoint of the Smoluchowski equation [117] and can be solved by a variety of numerical methods. The first moment of the off-rate distribution is τ_{off} which can be determined by intra-pore diffusion constant D and direct integration for an initial position x_0 as:

$$D\tau_{off}(x_0) = \left[\int_0^L dx \left(e^{\tilde{U}(x)} \int_0^x e^{-\tilde{U}(x')} dx' \right) \right] \left[\int_0^{x_0} e^{\tilde{U}(x')} dx' \right] \left[\int_0^L e^{\tilde{U}(x')} dx' \right]^{-1} - \int_0^{x_0} dx \left(e^{\tilde{U}(x)} \int_0^x e^{-\tilde{U}(x')} dx' \right) \quad (3)$$

In many cases, $U(x)$ can be parameterized by a very few quantities, each of which has a well-defined physical interpretation [118]. A minimum set of these, which was previously validated on long DNA molecules in solid-state nanopores [119], includes two parameters describing the modification of the bare charge density on the polyelectrolyte due to electroosmotic flow in the nanopore [120–122] and any parameters required to describe the entropy of confinement of the polyelectrolyte in the nanopore [123]. Additional terms can be added to deal with particular cases, such as post-translational modifications [101] or association with the membrane [104, 112].

For determining the effect of membrane lipids on α Syn binding strength and conformation, one of the more important terms in $U(x)$ is the membrane binding energy. This is modeled as an error function barrier with three parameters: the energy barrier height E_b , the position at which half the energy barrier has been overcome, x_b , and the width of the error function w_b , which is a measure of how gradually the unbinding process occurs. E_b is most closely related to the binding energy of a single molecule on the lipid membrane surface, while x_b is related to the accessibility of the C-terminal tail for capture into the VDAC nanopore and will be of particular importance in distinguishing among surface binding conformations of α Syn. The effect of E_b and x_b on the free energy profile is detailed in Figure 6 of [104]. Typical values of E_b are $15 k_B T$, which are largely consistent with the binding constants

determined by fluorescence correlation spectroscopy (FCS) measurements of α Syn binding to large unilamellar liposome membranes [91].

It should be noted that while the theory of the off-rate distribution appears to be independent of the nanopore used, the nanopore geometry affects the hydrodynamic resistance encountered by a polypeptide moving through the nanopore, and hence the intra-pore diffusion constant. The effects of the bulk vs. intra-pore diffusivities on the dynamics of molecule capture and release by a single nanopore were recently analyzed in a series of theoretical studies [124–126]. The geometry and the charge distribution on the walls of the pore also influence the magnitude of electroosmosis, which affects the effective charge density of the polypeptide. Additionally, one might imagine a position-dependent term for the interaction of the polypeptide charge density and that of the nanopore; the magnitude of this term can be estimated from the partition coefficient of charged vs. uncharged regions of α Syn in the VDAC nanopore [60] and is found to be weakly voltage-dependent and on the order of $1 k_B T$ at typical experimental voltages. This is a small correction to the electrical and membrane binding forces and is neglected in this discussion.

4. Effect of lipids on α Syn-VDAC binding kinetics

α Syn added to the planar membrane containing VDAC nanopore produces characteristic current fluctuations in milliseconds range at application of negative voltage from the side of α Syn addition in a lipid-dependent way. Examples of three typical experiments with VDAC1 reconstituted into the planar membranes made of three different lipid compositions are shown in Figure 4A. Two lipid mixtures have been chosen to mimic rat liver MOM composition where DOPC (PC) and DOPE (PE) make up 54 and 29% of the total lipid content, respectively [127] and the negatively charged DOPG (PG) represents a relatively high content (up to 20%) of the negatively charged lipid to which α Syn preferentially binds [84, 111]. The positively charged synthetic lipid DOTAP (TAP) was chosen as an oppositely charged lipid. 50% (mol/mol) of DOPG or DOTAP have been used in PC:PE (1:1, mol/mol) (PC/PE) mixtures. All lipids in these experiments have the same dioleoyl acyl chains to discriminate the effect of the lipid headgroup chemistry and charge on α Syn-VDAC interaction.

The lipid composition does not measurably affect the conductance of either the open or α Syn-blocked states (Figure 4A). By contrast, the differences in $k_{on} = \tau_{on}^{-1}$ and the distributions of t_{off} are striking and can be seen in three current traces obtained on single channels in the presence 10 nM of α Syn (Figure 4A and *Insets*). The k_{on} obtained in the negatively charged PG:PC:PE (2:1:1, mol:mol) (2PG/PC/PE) membranes is >10 times higher than in the positively charged TAP:PC:PE (2:1:1, mol/mol) (2TAP/PC/PE), with PC/PE membranes in between them (Figure 4B). The type of the lipid headgroup also affects the on-rate: the k_{on} in pure DOPE is ~10 times higher than in pure DOPC (Figure 4C). Cardiolipin (CL), a signature lipid of the MIM and found in residual amounts in the MOM [127], almost doubles the k_{on} when added at 20 mol% to the PC/PE mixture (Figure 4C), which could be accounted for by its negative charge and nonlamellar feature, but does not support the earlier proposed specificity of α -syn-CL binding [128].

The dependence of blockage times t_{off} (indicated by red arrows in Figure 4A) on lipid composition is visible even in the current traces (*insets*), but can be best seen by the t_{off} distributions in Figure 6A. Distributions of t_{off} obtained on the membranes with highest α Syn k_{on} —anionic, pure DOPE [92] (Figure 6A), or diphytanoylphosphatidylcholine (DPhPC) [18]—are well described by single exponential functions at all applied voltages [104]. In the membranes made of the lipids with low α Syn k_{on} —neutral DOPC, an equimolar PC/PE mixture (Figure 6A) and cationic 2TAP/PC/PE [92]—the t_{off} distributions cannot be described by a single exponent [104]. In PC/PE and pure DOPC, there are two well defined populations of t_{off} s separated by a factor of 20, such that the whole t_{off} distribution can be satisfactorily described by a sum of two single exponents with characteristic times $\tau_{off}^{(1)}$ and $\tau_{off}^{(2)}$ (Figure 6A). In cationic 2TAP/PC/PE membranes, the long-lasting t_{off} distribution is broad and requires more than two exponents to describe [104]. The occurrence of long-lasting $\tau_{off}^{(2)}$ increases with applied voltage from a minor, 10–20%, to a significant 50% fraction, depending on lipid composition [104] (Table 1).

5. Model of membrane-bound α Syn conformations

The results of the VDAC nanopore-based analysis of α Syn-lipid interactions are summarized in Table 1 [92, 104]. To characterize k_{on} , the capture rate at a single voltage ($V = -35$ mV) is chosen. This is justified because the slope of $\log_{10} k_{on}$ with voltage is the same for all lipid compositions (Figure 4B). Using energy landscape modeling (section 3.2), the complex behavior of τ_{off} can be reduced to membrane binding energy and the single geometric parameter, the penetration depth x_b . This is shown for each lipid composition in Figure 6C. Note that the penetration depth informs us of the residue *in the pore center* at the furthest penetration of the CTT into the nanopore. Due to the thickness of the membrane, the residues closest to x_b that could be responsible for membrane anchoring are at about +2 nm from the penetration depth. Thus, it is quite reasonable that α Syn residue F94 (at $x = 18.4$ nm) is membrane-associated on anionic membranes ($x_b \approx 15$ nm), as discussed in section 2.

Table 1 and Figure 6C show that the population of long-lived events, $\tau_{off}^{(2)}$, is characterized by a much larger penetration depth x_b . A physical model corresponding to this observation is shown in Figure 7. A shorter penetration depth corresponds to a membrane anchoring point that is near the CTT (starred positions in Figure 7), such that the CTT cannot fully penetrate the VDAC nanopore. This leads to faster retractions ($\tau_{off}^{(1)}$), but also allows increases in the applied voltage to destabilize membrane binding, leading to mostly translocation events at higher voltages. By contrast, a larger penetration depth suggests that the membrane anchoring point is further from the CTT. Under the applied voltage, the entire CTT can pass through the nanopore; the weakly charged region of α Syn is in the nanopore, the force acting on the trapped molecule is weaker, and membrane binding is not destabilized with increased voltage. At the voltages reported in the measurements, a translocation regime is not observed.

NMR measurements suggest [81] the presence of a distal binding conformation on anionic lipids such as that shown in the upper right panel of Figure 7. In the VDAC nanopore

measurements, however, $\tau_{off}^{(2)}$ is not observed at significant levels. A clue to the reason of this absence arises from the strong correlation between low k_{on} and the presence of $\tau_{off}^{(2)}$ (Table 1). This leads to the natural conclusion that proximal conformations, for which the CTT is pinned close to the membrane surface (but not bound to the surface, as for the cationic lipids (Figure 8B)), are more likely to be captured by the VDAC nanopore. In other words, the incidence of each molecular conformation observed by the VDAC nanopore is strongly biased toward molecular conformations that lead account for $\tau_{off}^{(1)}$. This bias is likely to be particularly significant on anionic lipids, for which electrostatic repulsion of the CTT from the membrane surface is strong; distal conformations may be still present, but their observation by the VDAC pore may be strongly repressed, so that the probability of capture is low. In the terms of Eq. (2), distal conformations add an additional term to ΔG_{on}^{\ddagger} that represents the free energy required to bring the polyanionic CTT close to the anionic lipid surface. As a corollary, for the lipid compositions in which $\tau_{off}^{(2)}$ is present in a measurable fraction, it is likely that a substantial majority of the surface-bound molecules are in the corresponding distal conformations, even if accounting for a minority of observed events. Future studies with engineered proteins may be required to quantify the efficiency of capture for different molecular conformations.

A complete model for different lipid types is shown in Figure 8; proximal and distal conformations are shown by solid and dashed lines, respectively. For nominally neutral lipids with zwitterionic headgroups, the propensity of α Syn to adopt primarily proximal or distal conformations depends on the headgroup species and the salt concentration. For PC/PE membranes at low salt, proximal conformations are favored. This is likely due to electrostatic interactions between the lysines of the membrane-binding domain and the membrane surface, which is slightly anionic [129–132]. At high salt concentrations, electrostatic interactions are reduced and distal conformations are favored. Interestingly, unlike DOPC lipids, DOPE lipids appear to produce proximal conformations, possibly because the smaller PE lipid headgroup allows stronger hydrophobic interactions between the valine-rich α Syn central domain and the membrane interior (Figure 8D). DPhPC behaves similarly to DOPE [101, 112], presumably due to the increased lipid spacing introduced by the acyl chain methylation. Distal conformations, by contrast, appear to be favored on cationic lipids and DOPC (Figure 8C, B). Note that crowding on the membrane surface may also favor distal conformations.

Remarkably, Table 1 shows that the binding energy of α Syn to the lipid surface, as measured either by energy landscape modeling or FCS, is not strongly predictive of the conformational landscape and hence of the propensity of α Syn to block VDAC. This highlights an important predictive limitation of dissociation constant measurements in this system.

6. Role of mitochondrial lipids in α Syn-VDAC interaction: physiological implications

In the preceding sections, we have reviewed the nanopore-based evidence for the effect of lipid composition on the ensemble of conformations adopted by α Syn bound to membranes.

These results confirm and complement a variety of previous studies indicating the interdependence of membrane composition and morphology for function and pathology of α Syn, as reviewed in [88]. The specific lipid content of the cytosolic membranes with which α Syn is found associated—plasma membrane [133], synaptic vesicles [134], or mitochondria [45, 52, 65, 135]—can modulate not only the quantity of membrane-bound α Syn but also its conformation. While a majority of studies are understandably focused on the effect of model and cell membranes on α Syn fibrillation potency, there is emerging interest in the conformations of lipid-associated α Syn monomers [81, 136, 137]. In our view, understanding how the conformation of α Syn molecules on membrane surfaces is related to function and pathologies of cell organelles is of great biological importance.

For the specific case of mitochondrial membranes, the lipid composition may play an additional role in modulating the α Syn-VDAC interaction and thus in regulation of metabolite fluxes through the VDAC channel (see discussion in [47]). Dynamic lipid exchange occurs at the contact sites between the two mitochondrial membranes and at the points of tight contact between mitochondria and other organelle membranes, such as endoplasmic or sarcoplasmic reticulum, or lysosomes that are known as mitochondrial associated membranes. The mitochondrial lipid composition is especially dynamic under oxidative stress [73–75] or apoptosis [72]. It is thus natural to speculate that the MOM lipid composition affects the ratio between α Syn populations in proximal and distal conformations at the MOM surface (Figure 7). In other words, lipid composition could affect the ratio between α Syn molecules in proximal conformations, which produce short-lived blockages but have a higher probability of entering mitochondria through the VDAC, and α Syn in distal conformations that produce longer-lived blockages and thus potentially could control metabolite flux through the VDAC more effectively (Figure 7) [104].

According to our working model, in normal mitochondrial physiology, α Syn regulates ATP/ADP fluxes through VDAC by dynamically blocking the pore [18]. In pathology such as α Syn overexpression, α Syn could enter mitochondria through VDAC and target electron transport complexes in the MIM causing their impairment. According to this model, an increase of anionic lipid content in the MOM could increase the population of α Syn in a membrane-proximal conformation, leading to higher translocation probability through VDAC (Figure 8A) and potentially to mitochondrial dysfunction. It is suggestive that under stress conditions such as apoptosis, the content of highly anionic and non-lamellar cardiolipin increases in the MOM [73] whereas it normally accounts for less than 1% of the total MOM lipid content [127]. Future experiments *in vitro* and *in vivo* will be required to determine if this model is relevant physiologically.

We have shown that the VDAC nanopore is sensitive to the effect of mitochondrial lipids on its cytosolic protein partners. By extension, this mitochondrial nanopore may be found to be useful for sensing the interactions of various cytosolic proteins such as glycolytic enzymes, hexokinase, cytoskeletal, neuronal, and Bcl-2 family pro- and anti-apoptotic proteins with the MOM [43, 138–144]. Notably, most of these cytosolic proteins, which execute their biological and pathological functions at the MOM platform, are weakly and transiently bound to the membrane.

7. Capture from the bulk versus capture from the membrane surface: experiments with α -Hemolysin nanopore

The idea of VDAC as a nanopore sensor is somewhat counterintuitive because under some conditions VDAC starts moving to its closed states at the applied transmembrane potentials as small as 30 mV. This should be compared with potentials of 100 mV or more necessary to gate many other β -barrel channels, especially those that find more regular use as sensors [145–149]. In addition, it was shown that changes in VDAC's environment, such as application of osmotic pressure [150], altering membrane lipid type [41], or decreasing solution pH [107], are able to increase the propensity of VDAC to gate under applied voltage. Even more importantly in the present context, it was demonstrated that the presence of certain negatively charged polymers that do not permeate VDAC can greatly increase the probability of gating transitions and thus VDAC's sensitivity to voltage [151]. For that reason, experiments with different nanopores as sensors for membrane-bound α Syn could be of great value.

Such experiments have been performed with another β -barrel channel, α -Hemolysin (α HL), where the crucial involvement of the membrane surface in α Syn interactions with membrane-imbedded nanopores was first demonstrated [152]. This extensively studied, prototypical nanopore [153–155] is formed as the result of self-assembly of seven α HL monomers into a mushroom-shaped structure (Figure 9). The nanopore, about 10 nm in length, is slightly anion-selective in 1M KCl solutions at neutral pH [156] and is characterized by a diameter which varies along the channel length, with the narrowest constriction of about 1.4 nm [153, 157]. Most notably, the α HL nanopore has a pronounced and functionally important asymmetry (Figure 9). The cap side of the nanopore, corresponding to the side of α HL addition in a reconstitution experiment (*cis*-side), is elevated by about 5 nm above the surface of the bilayer, while the opening on the other, stem side (*trans*-side), is flush with the membrane surface. The asymmetry, which is absent in the structure of membrane-embedded VDAC (Figure 1), makes the α HL nanopore an ideal probe for the discrimination between the bulk and membrane-surface-catalyzed processes.

One of the key findings reported by Gurnev et al. [152] was that addition of α Syn to the stem (*trans* in Figure 9) side of the nanopore results in an orders of magnitude greater on-rate of α Syn capture than that described in the initial publications on the interactions between α Syn and α HL [158, 159], where α Syn was added to the cap side of the pore. Indeed, capture events were readily observable when 50 nM α Syn was added to the *trans*-side of the membrane under transmembrane voltages of 40 mV relative to the side of α Syn addition, with the on-rate increasing by about 10-fold for a 20 mV increase in the applied voltage. For the *cis*-side addition of 50 nM α Syn, events were not observed at any voltages of either polarity; observation of rare events required a significantly higher α Syn concentration and voltages of 100 mV or more. This vast difference in the on-rates, exceeding three orders of magnitude if recalculated to the same voltages and concentrations, suggests that the protruding cap side of the channel cannot capture α Syn molecules from the membrane surface (Figure 9), but instead captures them from the bulk. In the context of equations (1) and (2), the value of ΔG_{on}^{\ddagger} is considerably larger for the membrane-bound

α Syn molecules that must stretch away from the membrane surface to reach the cap side of the channel, while the collision rate is much smaller for the molecules that do not adhere to the membrane surface.

The second finding of the study was that the on-rate for the surface-bound α Syn depended on the lipid species used for membrane formation, varying by more than 100-fold for the lipid compositions tested [152]. Similar to the findings with VDAC, the on-rate was shown to grow exponentially with the applied voltage (at least for relatively small voltages) and, in the range of small α Syn concentrations, to scale linearly with the concentration. At small α Syn concentrations it was found that for DPhPC membranes the on-rate constant was about 20 times higher than that for bilayers formed from the soybean polar lipid extract (PLE), with palmitoyl-phosphatidylcholine (POPC) bilayers demonstrating a 10-fold further reduction in the on-rate constant relative to that for PLE. Comparison of the capture rate dependences on α Syn concentration obtained from DPhPC and PLE bilayers revealed that, while they differ significantly, they both saturate at similar concentrations [152]. The dependences were best fit using simple binding isotherms with the characteristic concentrations of 30 and 32 nM for DPhPC and PLE, respectively. This observation led the authors to speculate that both DPhPC and PLE membranes bind α Syn in similar amounts, but PLE-bound molecules are somehow mostly incapacitated regarding their interaction with the channel. Indeed, the conjecture of the existence of different lipid-dependent conformations of α Syn, which differ in their ability to be trapped by a β -barrel nanopore, was, as described above, proved by further studies with the VDAC nanopore [92, 104].

The nanopore structures of VDAC and α HL are drastically different by the overall architecture, chemistry of the residues, and number of β -strands (19 and 14, respectively) involved in barrel formation (Figures 1 and 9). The stem side of the α HL nanopore, however, is similar to VDAC in that in both cases the pore opening is flush with the membrane surface. Besides, both nanopores have slight anion-selectivity in 1 M KCl and, while different in the total channel length, have similar dimensions of their narrowest constrictions and similar diameters of the *trans*-side opening. Given these similarities, it is instructive to compare the rates of α Syn capture by the α HL and VDAC nanopores. Such comparison suggests that the VDAC nanopore is orders-of-magnitude more proficient. Indeed, the *most catalyzing* membrane surface for the reaction of α HL with α Syn was found to be that of DPhPC bilayers, where the on-rate constant is about $8 \cdot 10^{-3} \text{ s}^{-1} \text{ nM}^{-1}$, measured at 40 mV applied voltage in 1 M KCl solutions at neutral pH (Figure 3C in [152]). This value is about $5 \cdot 10^3$ times lower than that for VDAC in DPhPC, other experimental conditions being the same [18]. Even for the *least catalyzing* lipid composition explored for VDAC, the 2TAP/PC/PE mixture, the on-rate constant is more than two orders of magnitude higher than the highest for α HL [92]. Specifically, extrapolated to 40 mV from the exponential fit of the data in the 25 mV to 37.5 mV range (Figure 1C in [92]), it is about $2.7 \text{ s}^{-1} \text{ nM}^{-1}$. This huge difference in the ability of the two nanopores to capture membrane-bound α Syn molecules reflects structural and electrostatic dissimilarities in the nanopore architectures. The main reason is probably in the channel conductance. VDAC, being nearly five times more conductive, upon application of the transmembrane voltage is expected to create five times stronger fields in the vicinity of its entrance. These fields act to capture α Syn molecules more efficiently. In the formalism of equations (1) and (2), the change in the on-rate is due to

the change in the contribution of the first term in the right-hand side of Eq. (2). An additional change in ΔG_{on}^{\ddagger} may also originate from the differences in the structures of the channel openings, which result in substantially different free energy barriers for the entry of the C-terminal tail of α Syn, accounted for by the second and third terms in right-hand side of Eq. (2). This conjecture is strongly supported by the two orders of magnitude difference in the on-rate of α Syn capture found for VDAC1 and VDAC3 isoforms [160].

In summary, experiments with α HL clearly demonstrated the crucial role of the membrane surface in the chain of events leading to α Syn interaction with β -barrel nanopores. Observation of the orders-of-magnitude lower probability of α Syn capture by the cap side of the α HL channel, which extends several nanometers into the bulk, compared to that of the capture by the stem side of the channel from the membrane surface, explicates the powerful catalyzing effect of the membrane interface. The data also support the notion of different conformations of membrane-bound α Syn, which are characterized by drastically different accessibility of its negatively charged C-terminus for the interaction with a membrane-embedded nanopore. Finally, comparison of the data obtained with VDAC and α HL suggests the importance of the fine structural and electrostatic features of a nanopore, including those that change electric field and its distributions at the nanopore entrance.

8. Conclusions

One of the important peculiarities of disordered proteins is their ability to undergo structural rearrangements upon binding/association with cell membranes. Moreover, their structure on the membrane surface strongly depends on membrane lipid composition, that is, on the nature of the acyl chains and the phospholipid headgroup charge, size, and hydration. These factors define membrane electrostatics and mechanical properties, such as membrane fluidity, bending and compressibility moduli, lipid spontaneous curvature, and, therefore, lipid packing stress. There are significant experimental limitations to identifying the structure of proteins that are weakly or transiently bound to the membrane, or that populate many different binding conformations. In the present review we demonstrate that a single-molecule nanopore-based approach is particularly useful in this case. Importantly, here the nanopore of our choice, VDAC, plays an unusual dual role: on the one hand, it is a nanoscale electromechanical device for probing the fine structural features of membrane-bound α Syn; on the other, it is the natural target of this cytosolic protein in mitochondria. VDAC as a nanopore probe turns out to be sensitive to the distribution of conformations adopted by different α Syn molecules on the same lipid surfaces. We show that the strength of α Syn binding to the membrane does not correlate in any simple way with its rates of capture or release by VDAC. Among many other membrane-specific effects, we indicate that the lipid-dependent association of the central domain of α Syn with the membrane surface appears to determine the availability of α Syn for capture by the VDAC nanopore and thus governs the overall interaction of α Syn with VDAC. We conclude that in addition to advocating VDAC as a promising nanopore sensor, our results have straightforward implications for the potential role of mitochondrial lipids in regulation of bioenergetics, stress response, and apoptosis.

Acknowledgments

The authors acknowledge contributions from Daniel Jacobs and Philip Gurnev to the experimental work, and thank Jennifer Lee for the kind gift of α Syn. Certain commercial materials, equipment, and instruments are identified in this work to describe the experimental procedure as completely as possible. In no case does such an identification imply a recommendation or endorsement by NIST, nor does it imply that the materials, equipment, or instrument identified are necessarily the best available for the purpose.

Funding sources

T.K.R. and S.M.B. were supported by the Intramural Research Program of the *Eunice Kennedy Shriver* National Institute of Child Health and Human Development (NICHD) of the National Institutes of Health (NIH).

References

- [1]. Colombini M, VDAC: The channel at the interface between mitochondria and the cytosol, *Mol Cell Biochem* 256(1–2) (2004) 107–115. [PubMed: 14977174]
- [2]. Lemasters JJ, Holmuhamedov E, Voltage-dependent anion channel (VDAC) as mitochondrial governor--thinking outside the box, *Biochimica et biophysica acta* 1762(2) (2006) 181–90. [PubMed: 16307870]
- [3]. Magri A, Messina A, Interactions of VDAC with Proteins Involved in Neurodegenerative Aggregation: An Opportunity for Advancement on Therapeutic Molecules, *Curr Med Chem* 24(40) (2017) 4470–4487. [PubMed: 28571556]
- [4]. Reina S, De Pinto V, Anti-Cancer Compounds Targeted to VDAC: Potential and Perspectives, *Curr Med Chem* 24(40) (2017) 4447–4469. [PubMed: 28554318]
- [5]. Leanza L, Checchetto V, Biasutto L, Rossa A, Costa R, Bachmann M, Zoratti M, Szabo I, Pharmacological modulation of mitochondrial ion channels, *Br J Pharmacol* 176(22) (2019) 4258–4283. [PubMed: 30440086]
- [6]. Shoshan-Barmatz V, Ben-Hail D, VDAC, a multi-functional mitochondrial protein as a pharmacological target, *Mitochondrion* 12(1) (2012) 24–34. [PubMed: 21530686]
- [7]. Shoshan-Barmatz V, Nahon-Crystal E, Shteinifer-Kuzmine A, Gupta R, VDAC1, mitochondrial dysfunction, and Alzheimer's disease, *Pharmacol Res* 131 (2018) 87–101. [PubMed: 29551631]
- [8]. Ujwal R, Cascio D, Colletier JP, Faham S, Zhang J, Toro L, Ping PP, Abramson J, The crystal structure of mouse VDAC1 at 2.3 angstrom resolution reveals mechanistic insights into metabolite gating, *Proc Natl Acad Sci USA* 105(46) (2008) 17742–17747. [PubMed: 18988731]
- [9]. Hiller S, Garces RG, Malia TJ, Orekhov VY, Colombini M, Wagner G, Solution structure of the integral human membrane protein VDAC-1 in detergent micelles, *Science* 321(5893) (2008) 1206–10. [PubMed: 18755977]
- [10]. Bayrhuber M, Meins T, Habeck M, Becker S, Giller K, Villinger S, Vornrhein C, Griesinger C, Zweckstetter M, Zeth K, Structure of the human voltage-dependent anion channel, *Proc Natl Acad Sci U S A* 105(40) (2008) 15370–15375. [PubMed: 18832158]
- [11]. Ujwal R, Cascio D, Colletier JP, Faham S, Zhang J, Toro L, Ping PP, Abramson J, The crystal structure of mouse VDAC1 at 2.3 angstrom resolution reveals mechanistic insights into metabolite gating, *Proc Natl Acad Sci U S A* 105(46) (2008) 17742–17747. [PubMed: 18988731]
- [12]. Song JM, Midson C, Blachly-Dyson E, Forte M, Colombini M, The sensor regions of VDAC are translocated from within the membrane to the surface during the gating processes, *Biophys J* 74(6) (1998) 2926–2944. [PubMed: 9635747]
- [13]. Thomas L, Blachly-Dyson E, Colombini M, Forte M, Mapping of residues forming the voltage sensor of the voltage-dependent anion-selective channel., *Proceedings of the National Academy of Sciences* 90(12) (1993) 5446–5449.
- [14]. Popp B, Court DA, Benz R, Neupert W, Lill R, The Role of the N and C Termini of Recombinant Neurospora Mitochondrial Porin in Channel Formation and Voltage-dependent Gating, *J Biol Chem* 271(23) (1996) 13593–13599. [PubMed: 8662769]
- [15]. Zachariae U, Schneider R, Briones R, Gattin Z, Demers J-P, Giller K, Maier E, Zweckstetter M, Griesinger C, Becker S, Benz R, Groot D, Bert L, Lange A, β -Barrel Mobility Underlies Closure

of the Voltage-Dependent Anion Channel, *Structure* 20(9) (2012) 1540–1549. [PubMed: 22841291]

- [16]. Gurnev PA, Rostovtseva TK, Bezrukov SM, Tubulin-blocked state of VDAC studied by polymer and ATP partitioning, *FEBS Lett.* 585(14) (2011) 2363–2366. [PubMed: 21722638]
- [17]. Colombini M, Pore-Size and Properties of Channels from Mitochondria Isolated from *Neurospora-Crassa*, *J Membrane Biol* 53(2) (1980) 79–84.
- [18]. Rostovtseva TK, Gurnev PA, Protchenko O, Hoogerheide DP, Yap TL, Philpott CC, Lee JC, Bezrukov SM, alpha-Synuclein Shows High Affinity Interaction with Voltage-dependent Anion Channel, Suggesting Mechanisms of Mitochondrial Regulation and Toxicity in Parkinson Disease, *J Biol Chem* 290(30) (2015) 18467–77. [PubMed: 26055708]
- [19]. Queralt-Martin M, Bergdoll L, Jacobs D, Bezrukov SM, Abramson J, Rostovtseva TK, Assessing the role of residue E73 and lipid headgroup charge in VDAC1 voltage gating, *Biochim Biophys Acta Bioenerg* 1860(1) (2019) 22–29. [PubMed: 30412693]
- [20]. Zambrowicz EB, Colombini M, Zero-current potentials in a large membrane channel: a simple theory accounts for complex behavior, *Biophys J* 65(3) (1993) 1093–100. [PubMed: 7694668]
- [21]. Krammer EM, Saidani H, Prevost M, Homble F, Origin of ion selectivity in *Phaseolus coccineus* mitochondrial VDAC, *Mitochondrion* 19 Pt B (2014) 206–13. [PubMed: 24742372]
- [22]. Schein SJ, Colombini M, Finkelstein A, Reconstitution in planar lipid bilayers of a voltage-dependent anion-selective channel obtained from *paramecium* mitochondria, *J Membr Biol* 30(2) (1976) 99–120. [PubMed: 1011248]
- [23]. Colombini M, Blachly-Dyson E, Forte M, VDAC, a channel in the outer mitochondrial membrane, *Ion Channels* 4 (1996) 169–202. [PubMed: 8744209]
- [24]. Colombini M, Structure and mode of action of a voltage dependent anion-selective channel (VDAC) located in the outer mitochondrial membrane, *Ann N Y Acad Sci* 341 (1980) 552–63. [PubMed: 6249159]
- [25]. Mlayeh L, Chatkaew S, Leonetti M, Homble F, Modulation of plant mitochondrial VDAC by phyosterols, *Biophys J* 99(7) (2010) 2097–106. [PubMed: 20923643]
- [26]. Gincel D, Zaid H, Shoshan-Barmatz V, Calcium binding and translocation by the voltage-dependent anion channel: a possible regulatory mechanism in mitochondrial function, *Biochem J* 358(Pt 1) (2001) 147–55. [PubMed: 11485562]
- [27]. Carbonara F, Popp B, Schmid A, Iacobazzi V, Genchi G, Palmieri F, Benz R, The role of sterols in the functional reconstitution of water-soluble mitochondrial porins from plants, *J Bioenerg Biomembr* 28(2) (1996) 181–9. [PubMed: 9132417]
- [28]. Ermishkin LN, Mirzabekov TA, Redistribution of the electric field within the pore contributes to the voltage-dependence of mitochondrial porin channel, *Biochim Biophys Acta* 1021(2) (1990) 161–8. [PubMed: 1689178]
- [29]. Rostovtseva TK, Bezrukov SM, ATP transport through a single mitochondrial channel, VDAC, studied by current fluctuation analysis, *Biophys J* 74(5) (1998) 2365–73. [PubMed: 9591663]
- [30]. Noskov SY, Rostovtseva TK, Chamberlin AC, Tejjido O, Jiang W, Bezrukov SM, Current state of theoretical and experimental studies of the voltage-dependent anion channel (VDAC), *Biochimica et biophysica acta* 1858(7 Pt B) (2016) 1778–90. [PubMed: 26940625]
- [31]. Rappaport SM, Tejjido O, Hoogerheide DP, Rostovtseva TK, Berezhkovskii AM, Bezrukov SM, Conductance hysteresis in the voltage-dependent anion channel, *Eur Biophys J* 44(6) (2015) 465–472. [PubMed: 26094068]
- [32]. Queralt-Martin M, Hoogerheide DP, Noskov SY, Berezhkovskii AM, Rostovtseva TK, Bezrukov SM, VDAC Gating Thermodynamics, but Not Gating Kinetics, Are Virtually Temperature Independent, *Biophys J* 119(12) (2020) 2584–2592. [PubMed: 33189678]
- [33]. Rostovtseva T, Colombini M, ATP flux is controlled by a voltage-gated channel from the mitochondrial outer membrane, *J Biol Chem* 271(45) (1996) 28006–8. [PubMed: 8910409]
- [34]. Noskov SY, Rostovtseva TK, Bezrukov SM, ATP Transport through VDAC and the VDAC-Tubulin Complex Probed by Equilibrium and Nonequilibrium MD Simulations, *Biochemistry-US* 52(51) (2013) 9246–9256.
- [35]. Tan W, Colombini M, VDAC closure increases calcium ion flux, *Biochimica et biophysica acta* 1768(10) (2007) 2510–5. [PubMed: 17617374]

- [36]. Rosencrans WM, Rajendran M, Bezrukov SM, Rostovtseva TK, VDAC regulation of mitochondrial calcium flux: From channel biophysics to disease, *Cell Calcium* 94 (2021) 102356. [PubMed: 33529977]
- [37]. Lemeshko VV, Electrical control of the cell energy metabolism at the level of mitochondrial outer membrane, *Biochim Biophys Acta Biomembr* 1863(1) (2021) 183493. [PubMed: 33132193]
- [38]. Rostovtseva TK, Tan W, Colombini M, On the role of VDAC in apoptosis: fact and fiction, *J Bioenerg Biomembr* 37(3) (2005) 129–42. [PubMed: 16167170]
- [39]. Mlayeh L, Krammer E-M, Léonetti M, Prévost M, Homblé F, The mitochondrial VDAC of bean seeds recruits phosphatidylethanolamine lipids for its proper functioning, *Biochim Biophys Acta - Bioenergetics* 1858(9) (2017) 786–794. [PubMed: 28666835]
- [40]. Queralt-Martín M, Bergdoll L, Jacobs D, Bezrukov SM, Abramson J, Rostovtseva TK, Assessing the role of residue E73 and lipid headgroup charge in VDAC1 voltage gating, *Biochim Biophys Acta - Bioenergetics* 1860(1) (2019) 22–29. [PubMed: 30412693]
- [41]. Rostovtseva TK, Kazemi N, Weinrich M, Bezrukov SM, Voltage gating of VDAC is regulated by nonlamellar lipids of mitochondrial membranes, *J Biol Chem* 281(49) (2006) 37496–506. [PubMed: 16990283]
- [42]. Rostovtseva TK, Bezrukov SM, VDAC regulation: role of cytosolic proteins and mitochondrial lipids, *J Bioenerg Biomembr* 40(3) (2008) 163–70. [PubMed: 18654841]
- [43]. Rostovtseva TK, Sheldon KL, Hassanzadeh E, Monge C, Saks V, Bezrukov SM, Sackett DL, Tubulin binding blocks mitochondrial voltage-dependent anion channel and regulates respiration, *Proceedings of the National Academy of Sciences* 105(48) (2008) 18746–18751.
- [44]. Maldonado EN, Patnaik J, Mullins MR, Lemasters JJ, Free Tubulin Modulates Mitochondrial Membrane Potential in Cancer Cells, *Cancer Res.* 70(24) (2011) 10192–10201.
- [45]. Rovini A, Gurnev PA, Beilina A, Queralt-Martín M, Rosencrans W, Cookson MR, Bezrukov SM, Rostovtseva TK, Molecular mechanism of olesoxime-mediated neuroprotection through targeting alpha-synuclein interaction with mitochondrial VDAC, *Cell Mol Life Sci* (2019).
- [46]. Monge C, Beraud N, Kuznetsov AV, Rostovtseva T, Sackett D, Schlattner U, Vendelin M, Saks VA, Regulation of respiration in brain mitochondria and synaptosomes: restrictions of ADP diffusion in situ, roles of tubulin, and mitochondrial creatine kinase, *Mol Cell Biochem* 318(1–2) (2008) 147–65. [PubMed: 18629616]
- [47]. Rostovtseva TK, Hoogerheide DP, Rovini A, Bezrukov SM, Lipids in Regulation of the Mitochondrial Outer Membrane Permeability, *Bioenergetics, and Metabolism*, in: Rostovtseva TK (Ed.), *Molecular Basis for Mitochondrial Signaling*, Springer International Publishing, Cham, 2017, pp. 185–215.
- [48]. Goedert M, Jakes R, Spillantini MG, The Synucleinopathies: Twenty Years On, *J Parkinsons Dis* 7(s1) (2017) S53–S71.
- [49]. Spillantini MG, Schmidt ML, Lee VM, Trojanowski JQ, Jakes R, Goedert M, Alpha-synuclein in Lewy bodies, *Nature* 388(6645) (1997) 839–40. [PubMed: 9278044]
- [50]. Kruger R, Muller T, Riess O, Involvement of alpha-synuclein in Parkinson's disease and other neurodegenerative disorders, *J Neural Transm (Vienna)* 107(1) (2000) 31–40. [PubMed: 10809401]
- [51]. Robotta M, Gerding HR, Vogel A, Hauser K, Schildknecht S, Karreman C, Leist M, Subramaniam V, Drescher M, Alpha-synuclein binds to the inner membrane of mitochondria in an alpha-helical conformation, *Chembiochem* 15(17) (2014) 2499–502. [PubMed: 25209675]
- [52]. Li WW, Yang R, Guo JC, Ren HM, Zha XL, Cheng JS, Cai DF, Localization of alpha-synuclein to mitochondria within midbrain of mice, *Neuroreport* 18(15) (2007) 1543–6. [PubMed: 17885598]
- [53]. Ludtmann MHR, Angelova PR, Horrocks MH, Choi ML, Rodrigues M, Baev AY, Berezhnov AV, Yao Z, Little D, Banushi B, Al-Menhali AS, Ranasinghe RT, Whiten DR, Yapom R, Dolt KS, Devine MJ, Gissen P, Kunath T, Jaganjac M, Pavlov EV, Klenerman D, Abramov AY, Gandhi S, alpha-synuclein oligomers interact with ATP synthase and open the permeability transition pore in Parkinson's disease, *Nat Commun* 9(1) (2018) 2293. [PubMed: 29895861]
- [54]. Parihar MS, Parihar A, Fujita M, Hashimoto M, Ghafourifar P, Alpha-synuclein overexpression and aggregation exacerbates impairment of mitochondrial functions by augmenting oxidative

- stress in human neuroblastoma cells, *Int J Biochem Cell Biol* 41(10) (2009) 2015–24. [PubMed: 19460457]
- [55]. Elkon H, Don J, Melamed E, Ziv I, Shirvan A, Offen D, Mutant and wild-type alpha-synuclein interact with mitochondrial cytochrome C oxidase, *J Mol Neurosci* 18(3) (2002) 229–38. [PubMed: 12059041]
- [56]. Devi L, Raghavendran V, Prabhu BM, Avadhani NG, Anandatheerthavarada HK, Mitochondrial import and accumulation of alpha-synuclein impair complex I in human dopaminergic neuronal cultures and Parkinson disease brain, *J Biol Chem* 283(14) (2008) 9089–100. [PubMed: 18245082]
- [57]. Chinta SJ, Mallajosyula JK, Rane A, Andersen JK, Mitochondrial alpha-synuclein accumulation impairs complex I function in dopaminergic neurons and results in increased mitophagy in vivo, *Neurosci Lett* 486(3) (2010) 235–9. [PubMed: 20887775]
- [58]. Nakamura K, Nemani VM, Azarbal F, Skibinski G, Levy JM, Egami K, Munishkina L, Zhang J, Gardner B, Wakabayashi J, Sesaki H, Cheng Y, Finkbeiner S, Nussbaum RL, Masliah E, Edwards RH, Direct membrane association drives mitochondrial fission by the Parkinson disease-associated protein alpha-synuclein, *J Biol Chem* 286(23) (2011) 20710–26. [PubMed: 21489994]
- [59]. Hoogerheide DP, Gurnev PA, Rostovtseva TK, Bezrukov SM, Mechanism of alpha-synuclein translocation through a VDAC nanopore revealed by energy landscape modeling of escape time distributions, *Nanoscale* (2016).
- [60]. Hoogerheide DP, Gurnev PA, Rostovtseva TK, Bezrukov SM, Real-Time Nanopore-Based Recognition of Protein Translocation Success, *Biophys J* 114(4) (2018) 772–776. [PubMed: 29338842]
- [61]. Rovini A, Gurnev PA, Beilina A, Queralt-Martin M, Rosencrans W, Cookson MR, Bezrukov SM, Rostovtseva TK, Molecular mechanism of olesoxime-mediated neuroprotection through targeting alpha-synuclein interaction with mitochondrial VDAC, *Cell Mol Life Sci* 77(18) (2020) 3611–3626. [PubMed: 31760463]
- [62]. Nussbaum RL, Genetics of Synucleinopathies, *Cold Spring Harb Perspect Med* 8(6) (2018).
- [63]. Barrett PJ, Timothy Greenamyre J, Post-translational modification of alpha-synuclein in Parkinson's disease, *Brain Res* 1628(Pt B) (2015) 247–253. [PubMed: 26080075]
- [64]. Zhang J, Li X, Li JD, The Roles of Post-translational Modifications on alpha-Synuclein in the Pathogenesis of Parkinson's Diseases, *Front Neurosci* 13 (2019) 381. [PubMed: 31057362]
- [65]. Cole NB, Dieuliis D, Leo P, Mitchell DC, Nussbaum RL, Mitochondrial translocation of alpha-synuclein is promoted by intracellular acidification, *Exp Cell Res* 314(10) (2008) 2076–89. [PubMed: 18440504]
- [66]. Schlame M, Greenberg ML, Biosynthesis, remodeling and turnover of mitochondrial cardiolipin, *Biochim Biophys Acta Mol Cell Biol Lipids* 1862(1) (2017) 3–7. [PubMed: 27556952]
- [67]. Sparagna GC, Chicco AJ, Murphy RC, Bristow MR, Johnson CA, Rees ML, Maxey ML, McCune SA, Moore RL, Loss of cardiac tetralinoleoyl cardiolipin in human and experimental heart failure, *Journal of lipid research* 48(7) (2007) 1559–70. [PubMed: 17426348]
- [68]. Aufschneider A, Kohler V, Diessl J, Peselj C, Carmona-Gutierrez D, Keller W, Buttner S, Mitochondrial lipids in neurodegeneration, *Cell and tissue research* (2016).
- [69]. Ribas V, Garcia-Ruiz C, Fernandez-Checa JC, Mitochondria, cholesterol and cancer cell metabolism, *Clinical and translational medicine* 5(1) (2016) 22. [PubMed: 27455839]
- [70]. Furt F, Moreau P, Importance of lipid metabolism for intracellular and mitochondrial membrane fusion/fission processes, *Int. J. Biochem. Cell. B* 41(10) (2009) 1828–1836.
- [71]. Murley A, Nunnari J, The Emerging Network of Mitochondria-Organellar Contacts, *Mol Cell* 61(5) (2016) 648–653. [PubMed: 26942669]
- [72]. Crimi M, Esposti MD, Apoptosis-induced changes in mitochondrial lipids, *Biochim. Biophys. Acta* 1813(4) (2011) 551–557. [PubMed: 20888373]
- [73]. Kagan VE, Borisenko GG, Tyurina YY, Tyurin VA, Jiang JF, Potapovich AI, Kini V, Amoscato AA, Fujii Y, Oxidative lipidomics of apoptosis: Redox catalytic interactions of cytochrome C with cardiolipin and phosphatidylserine, *Free Radical Bio. Med.* 37(12) (2004) 1963–1985. [PubMed: 15544916]

- [74]. Pamplona R, Membrane phospholipids, lipoxidative damage and molecular integrity: A causal role in aging and longevity, *Biochim. Biophys. Acta* 1777(10) (2008) 1249–1262. [PubMed: 18721793]
- [75]. Paradies G, Petrosillo G, Paradies V, Ruggiero FM, Mitochondrial dysfunction in brain aging: Role of oxidative stress and cardiolipin, *Neurochem. Int.* 58(4) (2011) 447–457. [PubMed: 21215780]
- [76]. Zhu M, Li J, Fink AL, The association of alpha-synuclein with membranes affects bilayer structure, stability, and fibril formation, *J Biol Chem* 278(41) (2003) 40186–97. [PubMed: 12885775]
- [77]. Grey M, Dunning CJ, Gaspar R, Grey C, Brundin P, Sparr E, Linse S, Acceleration of α -Synuclein Aggregation by Exosomes*, *J Biol Chem* 290(5) (2015) 2969–2982. [PubMed: 25425650]
- [78]. Braun AR, Lacy MM, Ducas VC, Rhoades E, Sachs JN, alpha-Synuclein-induced membrane remodeling is driven by binding affinity, partition depth, and interleaflet order asymmetry, *J Am Chem Soc* 136(28) (2014) 9962–72. [PubMed: 24960410]
- [79]. Jiang Z, de Messieres M, Lee JC, Membrane remodeling by alpha-synuclein and effects on amyloid formation, *J Am Chem Soc* 135(43) (2013) 15970–3. [PubMed: 24099487]
- [80]. Jiang Z, Flynn JD, Teague WE, Gawrisch K, Lee JC, Stimulation of α -synuclein amyloid formation by phosphatidylglycerol micellar tubules, *Biochimica et Biophysica Acta (BBA) - Biomembranes* 1860(9) (2018) 1840–1847. [PubMed: 29501608]
- [81]. Fusco G, De Simone A, Gopinath T, Vostrikov V, Vendruscolo M, Dobson CM, Veglia G, Direct observation of the three regions in alpha-synuclein that determine its membrane-bound behaviour, *Nat Commun* 5 (2014) 3827. [PubMed: 24871041]
- [82]. Ulmer TS, Bax A, Comparison of structure and dynamics of micelle-bound human alpha-synuclein and Parkinson disease variants, *J Biol Chem* 280(52) (2005) 43179–87. [PubMed: 16166095]
- [83]. Eliezer D, Kutluay E, Bussell R Jr., Browne G, Conformational properties of alpha-synuclein in its free and lipid-associated states, *J Mol Biol* 307(4) (2001) 1061–73. [PubMed: 11286556]
- [84]. Pfefferkorn CM, Jiang Z, Lee JC, Biophysics of alpha-synuclein membrane interactions, *Biochim Biophys Acta* 1818(2) (2012) 162–71. [PubMed: 21819966]
- [85]. El-Agnaf OM, Bodles AM, Guthrie DJ, Harriott P, Irvine GB, The N-terminal region of non-A beta component of Alzheimer's disease amyloid is responsible for its tendency to assume beta-sheet and aggregate to form fibrils, *Eur J Biochem* 258(1) (1998) 157–63. [PubMed: 9851705]
- [86]. Ulmer TS, Bax A, Cole NB, Nussbaum RL, Structure and dynamics of micelle-bound human alpha-synuclein, *J Biol Chem* 280(10) (2005) 9595–603. [PubMed: 15615727]
- [87]. Lokappa SB, Ulmer TS, α -Synuclein Populates Both Elongated and Broken Helix States on Small Unilamellar Vesicles, *J Biol Chem* 286(24) (2011) 21450–21457. [PubMed: 21524999]
- [88]. Kaur U, Lee JC, Membrane Interactions of α -Synuclein Probed by Neutrons and Photons, *Accounts of Chemical Research* (2021).
- [89]. Jiang Z, Heinrich F, McGlinchey RP, Gruschus JM, Lee JC, Segmental Deuteration of alpha-Synuclein for Neutron Reflectometry on Tethered Bilayers, *J Phys Chem Lett* 8(1) (2017) 29–34. [PubMed: 27936328]
- [90]. Jiang Z, Hess SK, Heinrich F, Lee JC, Molecular Details of α -Synuclein Membrane Association Revealed by Neutrons and Photons, *The Journal of Physical Chemistry B* 119(14) (2015) 4812–4823. [PubMed: 25790164]
- [91]. Middleton ER, Rhoades E, Effects of curvature and composition on alpha-synuclein binding to lipid vesicles, *Biophys J* 99(7) (2010) 2279–88. [PubMed: 20923663]
- [92]. Jacobs D, Hoogerheide DP, Rovini A, Jiang Z, Lee JC, Rostovtseva TK, Bezrukov SM, Probing Membrane Association of alpha-Synuclein Domains with VDAC Nanopore Reveals Unexpected Binding Pattern, *Sci Rep* 9(1) (2019) 4580. [PubMed: 30872688]
- [93]. Bezrukov SM, Vodyanoy I, Parsegian VA, Counting polymers moving through a single ion channel, *Nature* 370(6487) (1994) 279–281. [PubMed: 7518571]
- [94]. Coulter WA, Means for counting particles suspended in a fluid, US, 1953.

- [95]. Hoogerheide DP, Garaj S, Golovchenko JA, Probing Surface Charge Fluctuations with Solid-State Nanopores, *Phys Rev Lett* 102(25) (2009) 256804. [PubMed: 19659110]
- [96]. Kasianowicz JJ, Bezrukov SM, Protonation dynamics of the alpha-toxin ion channel from spectral analysis of pH-dependent current fluctuations, *Biophys J* 69(1) (1995) 94–105. [PubMed: 7545444]
- [97]. Deamer D, Akeson M, Branton D, Three decades of nanopore sequencing, *Nat Biotechnol* 34(5) (2016) 518–24. [PubMed: 27153285]
- [98]. Kasianowicz JJ, Bezrukov SM, On ‘three decades of nanopore sequencing’, *Nat Biotechnol* 34(5) (2016) 481–2. [PubMed: 27153275]
- [99]. Ouldali H, Sarthak K, Ensslen T, Piguet F, Manivet P, Pelta J, Behrends JC, Aksimentiev A, Oukhaled A, Electrical recognition of the twenty proteinogenic amino acids using an aerolysin nanopore, *Nat Biotechnol* 38(2) (2020) 176–181. [PubMed: 31844293]
- [100]. Thakur AK, Movileanu L, Real-time measurement of protein–protein interactions at single-molecule resolution using a biological nanopore, *Nat Biotechnol* 37(1) (2019) 96–101.
- [101]. Hoogerheide DP, Gurnev PA, Rostovtseva TK, Bezrukov SM, Effect of a post-translational modification mimic on protein translocation through a nanopore, *Nanoscale* 12(20) (2020) 11070–11078. [PubMed: 32400834]
- [102]. Finkelstein A, Proton-coupled protein transport through the anthrax toxin channel, *Philosophical Transactions of the Royal Society B: Biological Sciences* 364(1514) (2009) 209–215.
- [103]. Schiffmiller A, Anderson D, Finkelstein A, Ion selectivity of the anthrax toxin channel and its effect on protein translocation, *Journal of General Physiology* 146(2) (2015) 183–192.
- [104]. Hoogerheide DP, Rostovtseva TK, Jacobs D, Gurnev PA, Bezrukov SM, Tunable Electromechanical Nanopore Trap Reveals Populations of Peripheral Membrane Protein Binding Conformations, *ACS Nano* 15(1) (2021) 989–1001. [PubMed: 33369404]
- [105]. Willems K, Meervelt VV, Wloka C, Maglia G, Single-molecule nanopore enzymology, *Philosophical Transactions of the Royal Society B: Biological Sciences* 372(1726) (2017) 20160230.
- [106]. Mlayeh L, Krammer EM, Leonetti M, Prevost M, Homble F, The mitochondrial VDAC of bean seeds recruits phosphatidylethanolamine lipids for its proper functioning, *Biochim Biophys Acta Bioenerg* 1858(9) (2017) 786–794. [PubMed: 28666835]
- [107]. Teijido O, Rappaport SM, Chamberlin A, Noskov SY, Aguilera VM, Rostovtseva TK, Bezrukov SM, Acidification asymmetrically affects voltage-dependent anion channel implicating the involvement of salt bridges, *J Biol Chem* 289(34) (2014) 23670–82. [PubMed: 24962576]
- [108]. Bowen KA, Tam K, Colombini M, Evidence for titratable gating charges controlling the voltage dependence of the outer mitochondrial membrane channel, VDAC, *J Membr Biol* 86(1) (1985) 51–9. [PubMed: 2413210]
- [109]. Bezrukov SM, Ion Channels as Molecular Coulter Counters to Probe Metabolite Transport, *J Membrane Biol* 174(1) (2000) 1–13. [PubMed: 10741427]
- [110]. Smeets RMM, Keyser UF, Krapf D, Wu M-Y, Dekker NH, Dekker C, Salt Dependence of Ion Transport and DNA Translocation through Solid-State Nanopores, *Nano Lett* 6(1) (2006) 89–95. [PubMed: 16402793]
- [111]. Davidson WS, Jonas A, Clayton DF, George JM, Stabilization of alpha-synuclein secondary structure upon binding to synthetic membranes, *J Biol Chem* 273(16) (1998) 9443–9. [PubMed: 9545270]
- [112]. Hoogerheide DP, Gurnev PA, Rostovtseva TK, Bezrukov SM, Mechanism of alpha-synuclein translocation through a VDAC nanopore revealed by energy landscape modeling of escape time distributions, *Nanoscale* 9(1) (2017) 183–192. [PubMed: 27905618]
- [113]. Muthukumar M, Theory of capture rate in polymer translocation, *J Chem Phys* 132(19) (2010) 195101. [PubMed: 20499989]
- [114]. Kramers HA, Brownian motion in a field of force and the diffusion model of chemical reactions, *Physica* 7(4) (1940) 284–304.
- [115]. Hoogerheide DP, Lu B, Golovchenko JA, Pressure-Voltage Trap for DNA near a Solid-State Nanopore, *Acs Nano* 8(7) (2014) 7384–7391. [PubMed: 24933128]

- [116]. Chuang J, Kantor Y, Kardar M, Anomalous dynamics of translocation, *Phys Rev E* 65(1) (2001).
- [117]. van Kampen NG, *Stochastic processes in physics and chemistry*, 3rd ed., Elsevier, Amsterdam; Boston, 2007.
- [118]. Hoogerheide DP, PPDiffuse: A Quantitative Prediction Tool for Diffusion of Charged Polymers in a Nanopore, *J Res Natl Inst Stan* 125 (2020) 125018.
- [119]. Hoogerheide DP, Albertorio F, Golovchenko JA, Escape of DNA from a Weakly Biased Thin Nanopore: Experimental Evidence for a Universal Diffusive Behavior, *Phys Rev Lett* 111(24) (2013) 248301. [PubMed: 24483704]
- [120]. Keyser UF, Koeleman BN, van Dorp S, Krapf D, Smeets RMM, Lemay SG, Dekker NH, Dekker C, Direct force measurements on DNA in a solid-state nanopore, *Nat Phys* 2(7) (2006) 473–477.
- [121]. Lu B, Hoogerheide DP, Zhao Q, Yu DP, Effective driving force applied on DNA inside a solid-state nanopore, *Phys Rev E* 86(1) (2012).
- [122]. van Dorp S, Keyser UF, Dekker NH, Dekker C, Lemay SG, Origin of the electrophoretic force on DNA in solid-state nanopores, *Nature Physics* 5(5) (2009) 347–351.
- [123]. Rostovtseva TK, Gurnev PA, Hoogerheide DP, Rovini A, Sirajuddin M, Bezrukov SM, Sequence diversity of tubulin isoforms in regulation of the mitochondrial voltage-dependent anion channel, *J Biol Chem* 293(28) (2018) 10949–10962. [PubMed: 29777059]
- [124]. Berezhkovskii AM, Bezrukov SM, Blocker escape kinetics from a membrane channel analyzed by mapping blocker diffusive dynamics onto a two-site model, *J Chem Phys* 150(19) (2019) 194103. [PubMed: 31117787]
- [125]. Berezhkovskii AM, Bezrukov SM, Capturing single molecules by nanopores: measured times and thermodynamics, *Phys Chem Chem Phys* 23(2) (2021) 1610–1615. [PubMed: 33410847]
- [126]. Berezhkovskii AM, Dagdug L, Bezrukov SM, Two-site versus continuum diffusion model of blocker dynamics in a membrane channel: Comparative analysis of escape kinetics, *J Chem Phys* 151 (2019) 054113.
- [127]. Horvath SE, Daum G, Lipids of mitochondria, *Prog Lipid Res* 52(4) (2013) 590–614. [PubMed: 24007978]
- [128]. Zigoneanu IG, Yang YJ, Krois AS, Haque E, Pielak GJ, Interaction of alpha-synuclein with vesicles that mimic mitochondrial membranes, *Biochim Biophys Acta* 1818(3) (2012) 512–9. [PubMed: 22155643]
- [129]. Chibowski E, Szczes A, Zeta potential and surface charge of DPPC and DOPC liposomes in the presence of PLC enzyme, *Adsorption* 22(4–6) (2016) 755–765.
- [130]. Morini MA, Sierra MS, Pedroni VI, Alarcon LM, Appignanesi GA, Disalvo EA, Influence of temperature, anions and size distribution on the zeta potential of DMPC, DPPC and DMPE lipid vesicles, *Colloid Surf. B-Biointerfaces* 131 (2015) 54–58.
- [131]. Smith MC, Crist RM, Clogston JD, McNeil SE, Zeta potential: a case study of cationic, anionic, and neutral liposomes, *Anal Bioanal Chem* 409(24) (2017) 5779–5787. [PubMed: 28762066]
- [132]. Michalak DJ, Lösche M, Hoogerheide DP, Charge Effects Provide Ångström-Level Control of Lipid Bilayer Morphology on Titanium Dioxide Surfaces, *Langmuir* 37(13) (2021) 3970–3981. [PubMed: 33761262]
- [133]. Kaur U, Lee JC, Unroofing site-specific alpha-synuclein-lipid interactions at the plasma membrane, *Proc Natl Acad Sci U S A* 117(32) (2020) 18977–18983. [PubMed: 32719116]
- [134]. Clayton DF, George JM, The synucleins: a family of proteins involved in synaptic function, plasticity, neurodegeneration and disease, *Trends Neurosci* 21(6) (1998) 249–54. [PubMed: 9641537]
- [135]. Nakamura K, Nemani VM, Wallender EK, Kaehlcke K, Ott M, Edwards RH, Optical reporters for the conformation of alpha-synuclein reveal a specific interaction with mitochondria, *The Journal of neuroscience : the official journal of the Society for Neuroscience* 28(47) (2008) 12305–17.
- [136]. Kaur U, Lee JC, Membrane Interactions of alpha-Synuclein Probed by Neutrons and Photons, *Acc Chem Res* 54(2) (2021) 302–310. [PubMed: 33415971]

- [137]. Theillet FX, Binolfi A, Bekei B, Martorana A, Rose HM, Stuver M, Verzini S, Lorenz D, van Rossum M, Goldfarb D, Selenko P, Structural disorder of monomeric alpha-synuclein persists in mammalian cells, *Nature* 530(7588) (2016) 45–50. [PubMed: 26808899]
- [138]. Al Jamal JA, Involvement of porin N, N-dicyclohexylcarbodiimide-reactive domain in hexokinase binding to the outer mitochondrial membrane, *Protein J* 24 (2005) 1–8. [PubMed: 15756812]
- [139]. Magri A, Belfiore R, Reina S, Tomasello MF, Di Rosa MC, Guarino F, Leggio L, De Pinto V, Messina A, Hexokinase I N-terminal based peptide prevents the VDAC1-SOD1 G93A interaction and re-establishes ALS cell viability, *Sci Rep* 6 (2016) 34802. [PubMed: 27721436]
- [140]. Gouarne C, Giraudon-Paoli M, Seimandi M, Biscarrat C, Tardif G, Pruss RM, Bordet T, Olesoxime protects embryonic cortical neurons from camptothecin intoxication by a mechanism distinct from BDNF, *Br J Pharmacol* 168(8) (2013) 1975–88. [PubMed: 23278424]
- [141]. Gonzalvez F, Schug ZT, Houtkooper RH, MacKenzie ED, Brooks DG, Wanders RJ, Petit PX, Vaz FM, Gottlieb E, Cardiolipin provides an essential activating platform for caspase-8 on mitochondria, *J Cell Biol* 183(4) (2008) 681–96. [PubMed: 19001123]
- [142]. Yethon JA, Epand RF, Leber B, Epand RM, Andrews DW, Interaction with a membrane surface triggers a reversible conformational change in Bax normally associated with induction of apoptosis, *The Journal of biological chemistry* 278(49) (2003) 48935–41. [PubMed: 14522999]
- [143]. McNally MA, Soane L, Roelofs BA, Hartman AL, Hardwick JM, The N-terminal helix of Bcl-xL targets mitochondria, *Mitochondrion* 13(2) (2013) 119–24. [PubMed: 23333404]
- [144]. Renault TT, Teijido O, Antonsson B, Dejean LM, Manon S, Regulation of Bax mitochondrial localization by Bcl-2 and Bcl-x(L): keep your friends close but your enemies closer, *Int J Biochem Cell Biol* 45(1) (2013) 64–7. [PubMed: 23064052]
- [145]. Van Gelder P, Saint N, Phale P, Eppens EF, Prilipov A, van Boxtel R, Rosenbusch JP, Tommassen J, Voltage sensing in the PhoE and OmpF outer membrane porins of *Escherichia coli*: role of charged residues, *Journal of molecular biology* 269(4) (1997) 468–72. [PubMed: 9217251]
- [146]. Bainbridge G, Gokce I, Lakey JH, Voltage gating is a fundamental feature of porin and toxin beta-barrel membrane channels, *FEBS Lett* 431(3) (1998) 305–8. [PubMed: 9714531]
- [147]. Derrington IM, Butler TZ, Collins MD, Manrao E, Pavlenok M, Niederweis M, Gundlach JH, Nanopore DNA sequencing with MspA, *Proc Natl Acad Sci U S A* 107(37) (2010) 16060–5. [PubMed: 20798343]
- [148]. Mohammad MM, Iyer R, Howard KR, McPike MP, Borer PN, Movileanu L, Engineering a rigid protein tunnel for biomolecular detection, *J Am Chem Soc* 134(22) (2012) 9521–31. [PubMed: 22577864]
- [149]. Bogard A, Abatchev G, Hutchinson Z, Ward J, Finn PW, McKinney F, Fologea D, Lysenin Channels as Sensors for Ions and Molecules, *Sensors (Basel)* 20(21) (2020).
- [150]. Zimmerberg J, Parsegian VA, Polymer Inaccessible Volume Changes during Opening and Closing of a Voltage-Dependent Ionic Channel, *Nature* 323(6083) (1986) 36–39. [PubMed: 2427958]
- [151]. Mangan PS, Colombini M, Ultrasteep voltage dependence in a membrane channel, *Proc Natl Acad Sci U S A* 84(14) (1987) 4896–900. [PubMed: 2440034]
- [152]. Gurnev PA, Yap TL, Pfeifferkorn CM, Rostovtseva TK, Berezhkovskii AM, Lee JC, Parsegian VA, Bezrukov SM, Alpha-synuclein lipid-dependent membrane binding and translocation through the alpha-hemolysin channel, *Biophys J* 106(3) (2014) 556–65. [PubMed: 24507596]
- [153]. Song L, Hobaugh MR, Shustak C, Cheley S, Bayley H, Gouaux JE, Structure of staphylococcal alpha-hemolysin, a heptameric transmembrane pore, *Science* 274(5294) (1996) 1859–66. [PubMed: 8943190]
- [154]. Gurnev PA, Nestorovich EM, Channel-forming bacterial toxins in biosensing and macromolecule delivery, *Toxins (Basel)* 6(8) (2014) 2483–540. [PubMed: 25153255]
- [155]. Gu LQ, Braha O, Conlan S, Cheley S, Bayley H, Stochastic sensing of organic analytes by a pore-forming protein containing a molecular adapter, *Nature* 398(6729) (1999) 686–90. [PubMed: 10227291]

- [156]. Krasilnikov OV, Sabirov RZ, Ion transport through channels formed in lipid bilayers by Staphylococcus aureus alpha-toxin, *Gen Physiol Biophys* 8(3) (1989) 213–22. [PubMed: 2475386]
- [157]. Merzlyak PG, Yuldasheva LN, Rodrigues CG, Carneiro CM, Krasilnikov OV, Bezrukov SM, Polymeric nonelectrolytes to probe pore geometry: application to the alpha-toxin transmembrane channel, *Biophys J* 77(6) (1999) 3023–33. [PubMed: 10585924]
- [158]. Madampage C, Tavassoly O, Christensen C, Kumari M, Lee JS, Nanopore analysis: An emerging technique for studying the folding and misfolding of proteins, *Prion* 6(2) (2012) 116–23. [PubMed: 22421211]
- [159]. Wang HY, Gu Z, Cao C, Wang J, Long YT, Analysis of a single alpha-synuclein fibrillation by the interaction with a protein nanopore, *Anal Chem* 85(17) (2013) 8254–61. [PubMed: 23899046]
- [160]. Queralt-Martin M, Bergdoll L, Tejjido O, Munshi N, Jacobs D, Kuszak AJ, Protchenko O, Reina S, Magri A, De Pinto V, Bezrukov SM, Abramson J, Rostovtseva TK, A lower affinity to cytosolic proteins reveals VDAC3 isoform-specific role in mitochondrial biology, *J Gen Physiol* 152(2) (2020) e201912501. [PubMed: 31935282]

Highlights

- The voltage-dependent anion channel (VDAC) acts as both ion channel and nanopore
- As an ion channel VDAC is regulated by membrane-bound α -Synuclein (α Syn)
- As a nanopore VDAC allows electro-mechanical probing of membrane-bound proteins
- Lipid composition determines α Syn's surface density and conformational ensembles
- α Syn surface conformation defines rates of insertion into and release from VDAC

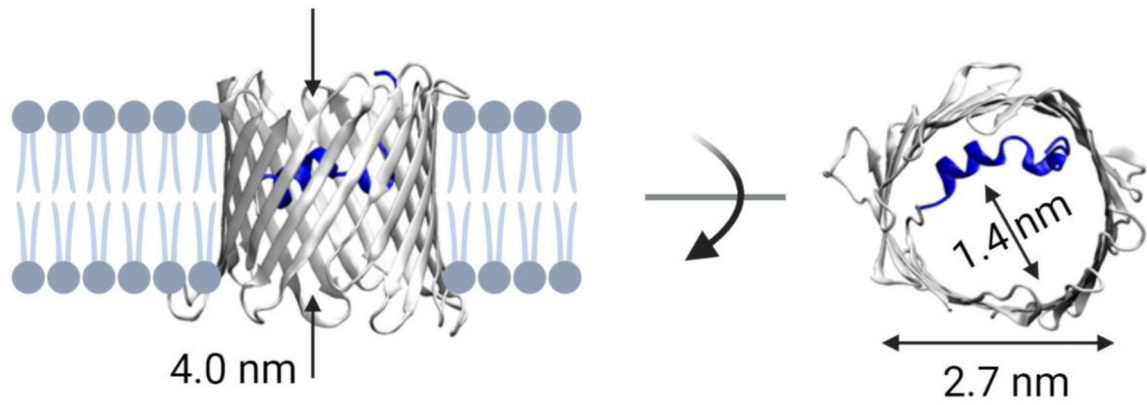


Figure 1. Structure of VDAC. Side and top view of mouse VDAC1 (mVDAC1, PDB ID: 3EMN). The elongated pore constriction is formed by the N-terminal α -helix (shown in dark blue) near the pore center. Created with [Biorender.com](https://biorender.com).

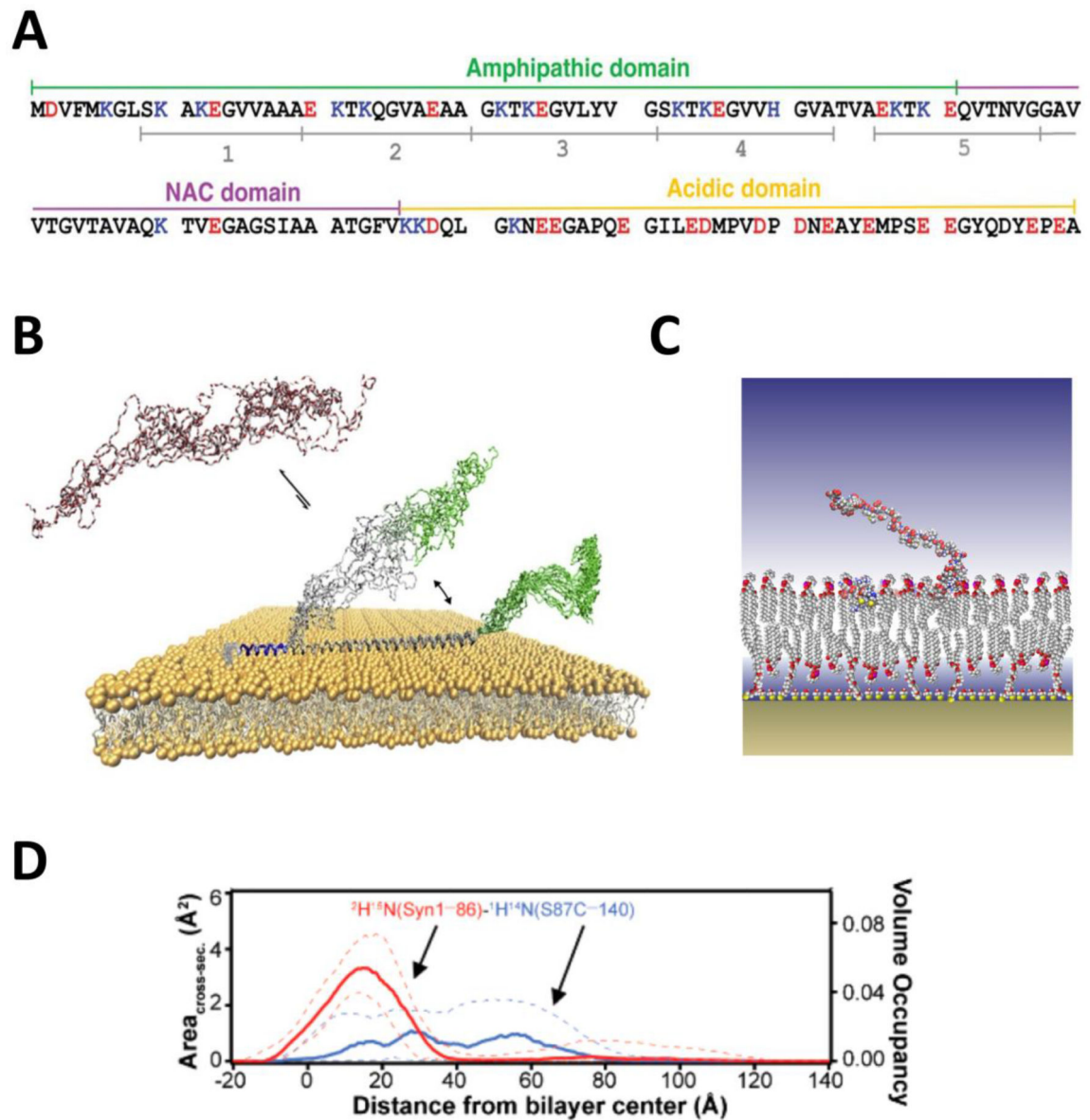


Figure 2.

Membrane-bound structure of α Syn. (A) Amino acid sequence of α Syn. Adapted with permission from Robyn Croke et al, In: “Protein Science”, Wiley Online Library. V. 20 (2), pp 256–269, Copyright © 2010 The Protein Society. The N-terminal region responsible for membrane interaction comprises both the amphipathic and the central (NAC) domains. The polyanionic C-terminal tail is responsible for interaction with the VDAC nanopore. (B) Solution and solid-state NMR derived structure of α Syn on anionic bilayers showing three distinct regions: a persistent helical region (blue); a transient binding domain (gray), which is helical when bound and disordered when unbound; and the C-terminal tail (green), which is only weakly associated with the lipid surface. Adapted with permission from Fusco et al, *Nat. Commun.* (2014). Copyright 2017 Elsevier. (C) Low-resolution structure of α Syn embedded in POPC/POPA bilayers. (D) Volume occupancy and cross-section area of the

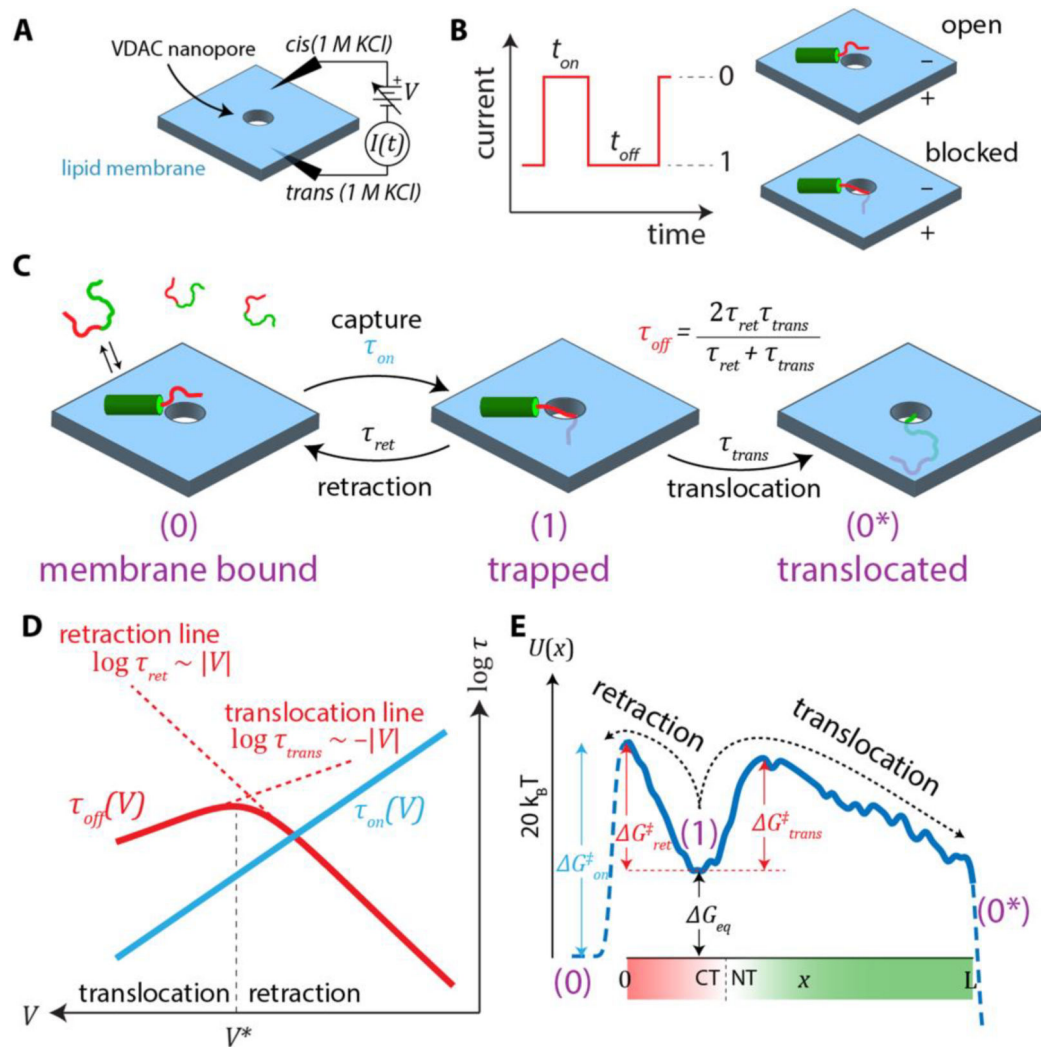
deuterated residues 1–86 (red) and protiated residues 87–140 (blue). Segmental deuteration, in combination with contrast variation, provides a domain-level view of the protein-lipid complex. Dashed lines show 68% confidence intervals. Adapted with permission from Jiang et al, *J. Phys. Chem. Lett.* (2017). Copyright © 2016 American Chemical Society.

Author Manuscript

Author Manuscript

Author Manuscript

Author Manuscript

**Figure 3.**

Nanopore-based analysis of surface-bound α Syn. (A) Schematic of a generic nanopore measurement. (B) An applied voltage produces an ionic current through the nanopore. If an analyte is drawn into the nanopore, it causes transient current blockages, or “events”, that are characterized by their onset time, t_{on} , and duration, t_{off} . (C) Reaction scheme of the nanopore- α Syn interaction. Once captured, the α Syn leaves the nanopore either by retraction or translocation, thus restoring the ionic current to its unblocked level. (D) Typical voltage dependences of the average rates. The average event duration, τ_{off} , has a biphasic dependence on voltage that indicates the transition from primarily retraction events to primarily translocation events. (E) Free energy landscape governing the reaction scheme in (C). The “reaction coordinate” x denotes the length of α Syn that has threaded into the VDAC nanopore past the constriction. The trapped state (1) is a metastable state that is an electromechanical trap formed by the opposite action of the electric field on the charged C-terminal domain (CT; shown in red) and the N-terminal domain (NT; shown in green) lipid-associated anchor.

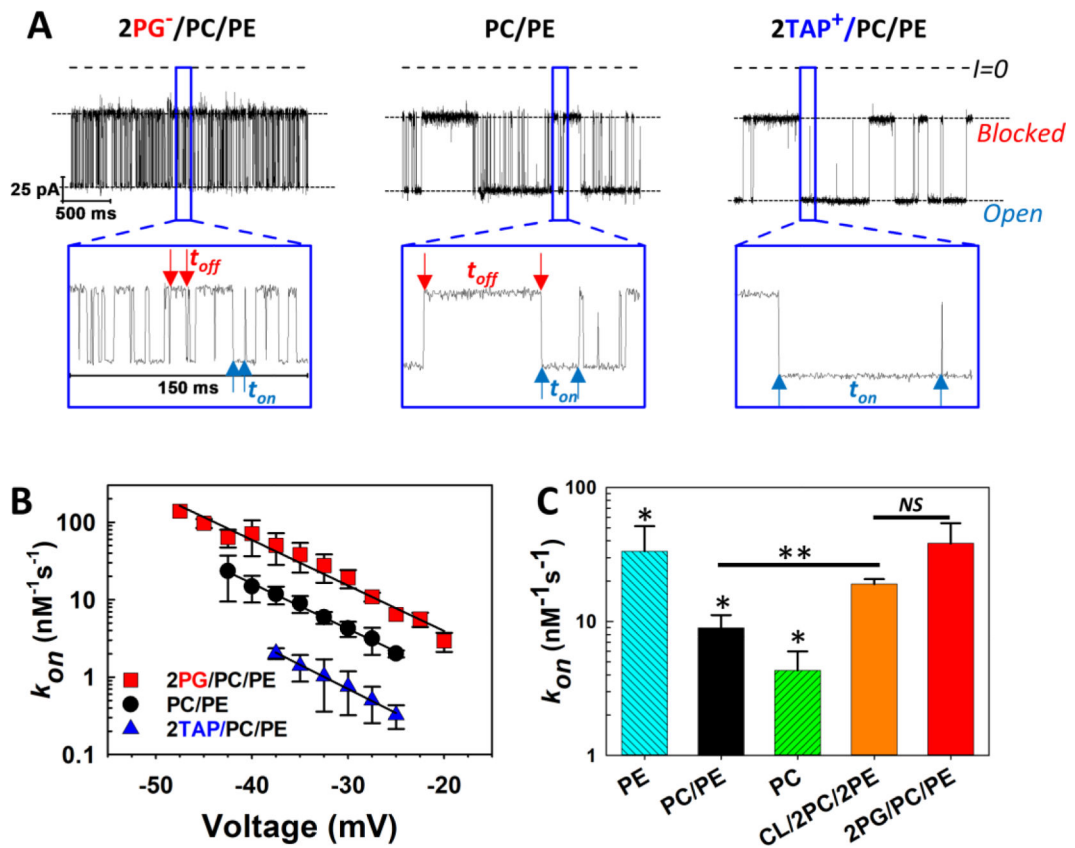


Figure 4.

The kinetics of α Syn blockage of VDAC strongly depend on membrane lipid composition. (A) Records of ion currents through single VDAC1 channels reconstituted into planar bilayers formed from DOPG:DOPC:DOPE (2:1:1, mol:mol) (2PG/PC/PE) (*left trace*), DOPC:DOPE (1:1, mol:mol) (PC/PE) (*middle traces*), and DOTAP:DOPC:DOPE (2:1:1, mol:mol) (2TAP/PC/PE) (*right trace*) obtained at -35 mV applied voltage. Individual, time-resolved blockage events can be seen in the *insets*, which show fragments of current records at a finer time scale. Horizontal dotted lines indicate VDAC open and blocked states; dashed lines indicate zero current. Blue arrows indicate durations of the open state, t_{on} , and red arrows show blocked state durations, t_{off} . Both parameters of blockage events visibly depend on lipid composition. Current traces were digitally filtered using a 5 kHz lowpass Bessel filter for presentation. (B) Voltage dependences of the rate of capture, k_{on} , obtained in three lipid compositions. The k_{on} of the α Syn-VDAC interaction increases in the presence of anionic and nonlamellar lipids. Error bars show 68% confidence intervals. (C) Summary of results for k_{on} obtained in DOPE (PE), PC/PE, DOPC (PC), Cardiolipin:DOPC:DOPE (1:2:2) (CL/2PC/2PE), and 2PG/PC/PE membranes at -35 mV applied voltage. All data were obtained in the presence of 10 nM of α Syn in the *cis* compartment in 1 M KCl at pH 7.4. Error bars show 68% confidence intervals. Adapted with permission from Jacobs et al. *Sci. Reports* (2019). Copyright © 2019 Springer Nature.

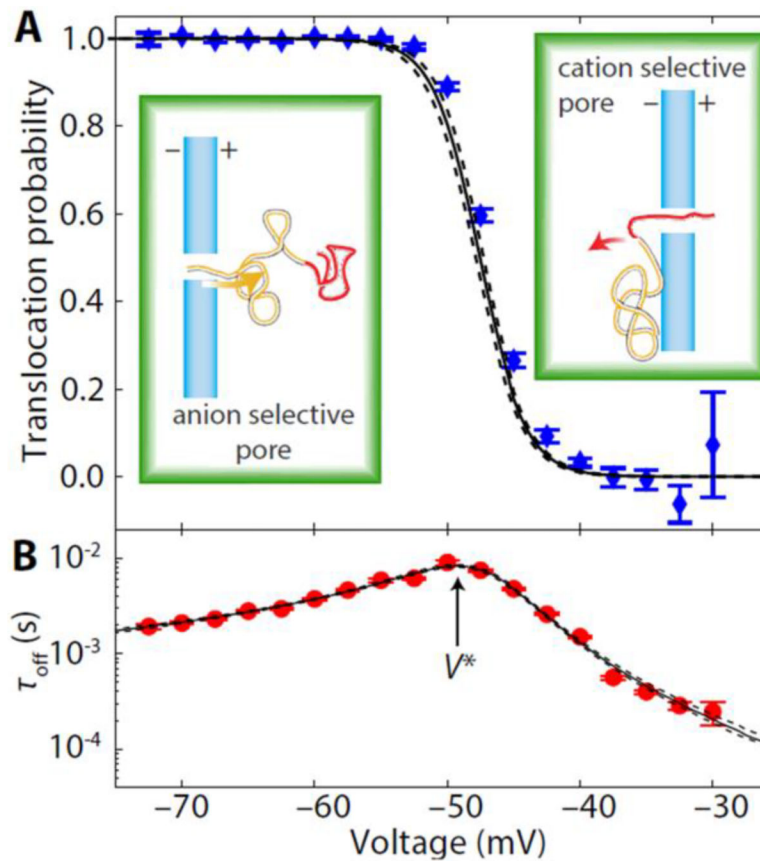


Figure 5.

Determination of the relationship between the biphasic voltage dependence of τ_{off} and the translocation probability. (A) The fraction of α Syn molecules that translocate through a VDAC pore transitions sharply from zero to unity near the turnover voltage V^* , where (B) the voltage-dependence of τ_{off} reverses slope. The solid and dashed lines in (B) are the median and 95% confidence interval, respectively, of an energy landscape model optimized to the observed τ_{off} ; this model accurately predicts the translocation probability and its 95% confidence interval (solid and dashed lines, respectively) in (A). Error bars are 68% confidence intervals calculated using bootstrap resampling. Adapted with permission from Hoogerheide et al. *Biophys. J.* (2018). Copyright © 2018, Elsevier.

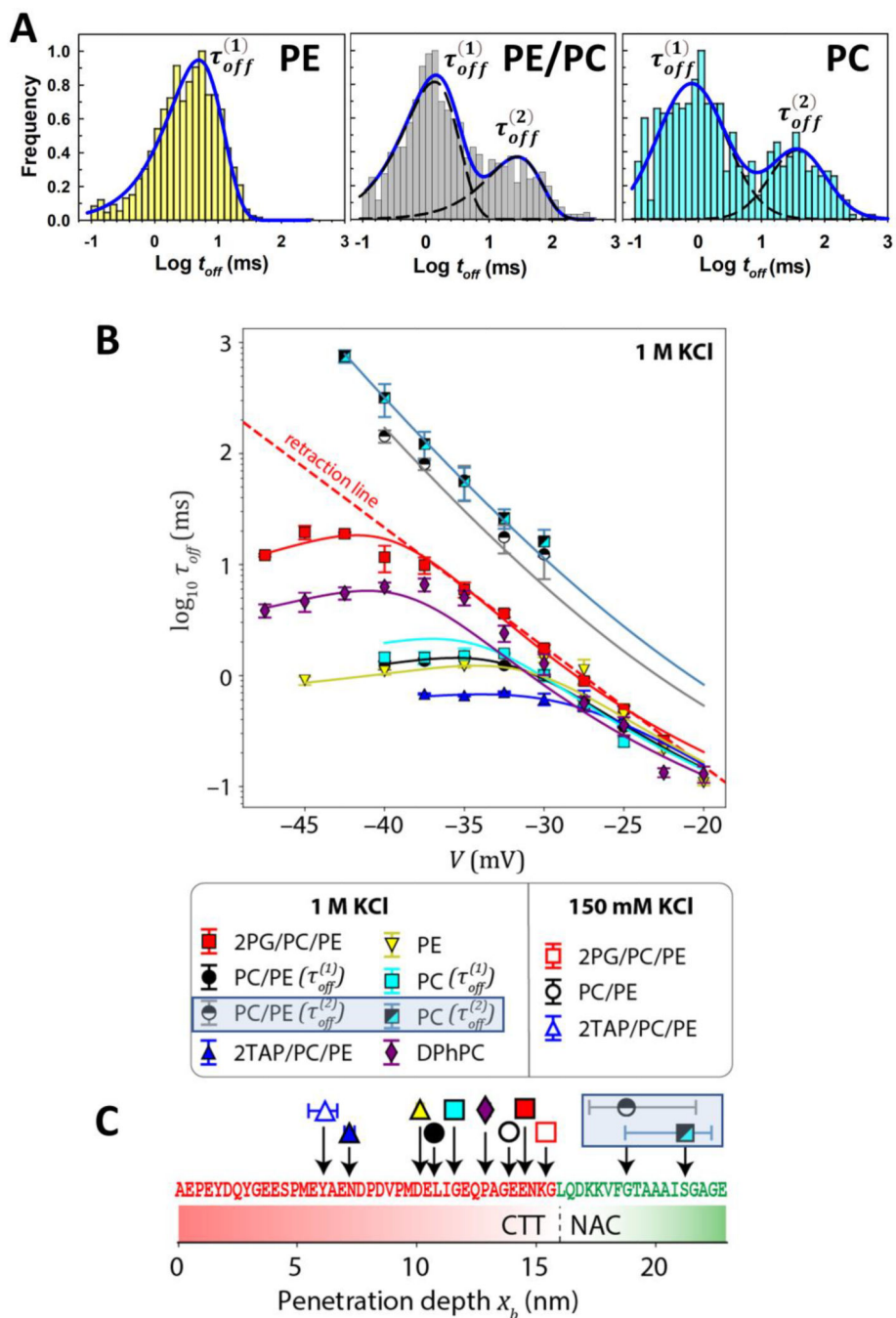


Figure 6. Lipid-dependent features of τ_{off} . (A) Distributions of t_{off} at $V = -35$ mV shows a single characteristic time scale, $\tau_{off}^{(1)}$, for DOPE lipids. At higher potentials, a second, slower time scale, $\tau_{off}^{(2)}$, is apparent in PC/PE and pure DOPC membranes. (B) For all lipid compositions, $\tau_{off}^{(1)}$ shows the characteristic transition from retraction to translocation; this transition is not observed for $\tau_{off}^{(2)}$ in PC/PE and DOPC lipids. The solid lines are model predictions with the optimized energy landscapes, $U(x)$, with only two free parameters per

curve. Error bars represent 68% confidence intervals. (C) Penetration depth obtained from the optimization for different lipid compositions. The depth represents the furthest residue that can penetrate the nanopore before deeper penetration is prevented by the membrane anchor. Error bars represent 95% confidence intervals and where not visible are smaller than the size of the data marker. Adapted with permission from Hoogerheide et al. *ACS Nano* (2021). Copyright © 2021, American Chemical Society.

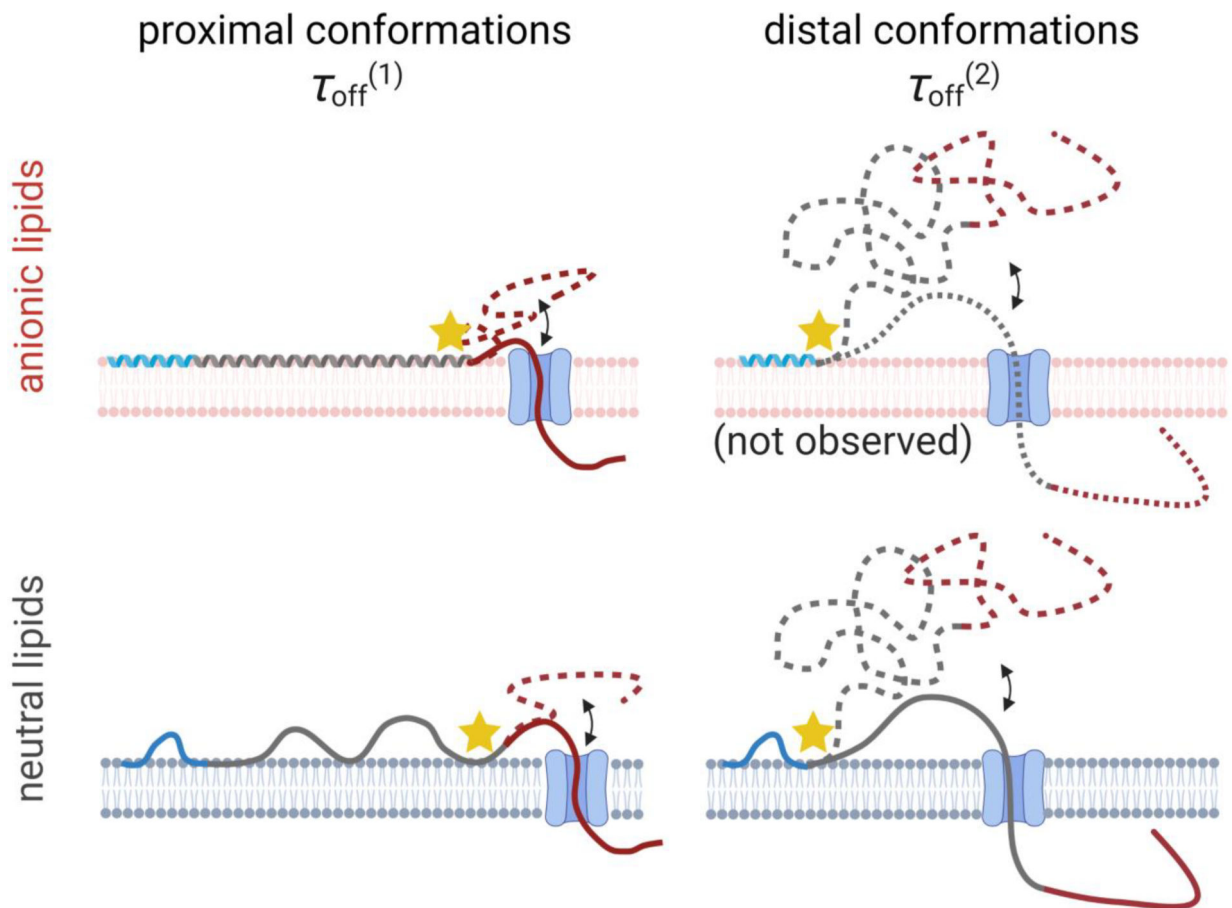
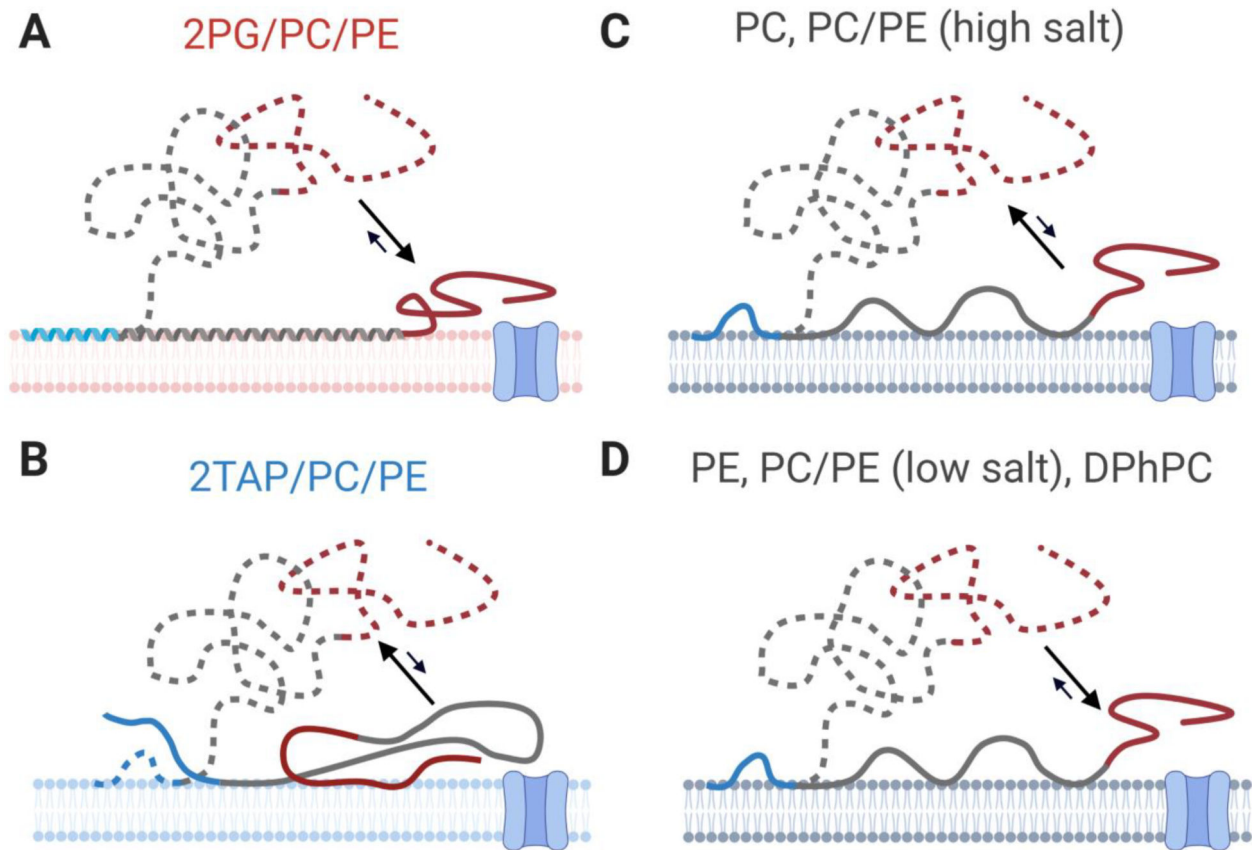


Figure 7.

Model of the possible α Syn conformations responsible for the different observed τ_{off} : The blue region of α Syn corresponds to the persistently membrane-bound domain identified by Fusco et al. [81] (Fig. 2B); the dynamic center region is shown in gray; and the CTT is shown in red. In each conformation, the position closest to the CTT that is pinned to the lipid membrane is shown with a star. For “proximal” membrane-bound conformations, where the pinning region extends near the CTT, which is constrained to be close to the membrane surface, $\tau_{off}^{(1)}$ is observed. For “distal” conformations, where the pinning region is further away from the CTT, allowing the CTT to float further from the membrane surface but also to penetrate entirely through the VDAC nanopore once captured, $\tau_{off}^{(2)}$ is observed.

Created with [Biorender.com](https://www.biorender.com).

**Figure 8.**

Model of binding conformations adopted by α Syn on membranes of different lipid compositions. Proximal conformations, which are readily captured and lead to short blockages of VDAC ($\tau_{off}^{(1)}$), are shown in solid lines; distal conformations, which are less available to the VDAC pore but have longer lifetimes ($\tau_{off}^{(2)}$), are shown by dashed lines.

Arrows reflect upon relative populations rather than dynamic equilibrium. (A) On anionic lipids, VDAC nanopore-based measurements are consistent with binding conformations observed by NMR. Distal conformations, however, are not observed. (B) In the proximal conformations on cationic membranes, the C-terminal domain is closely associated with the lipid surface. Distal conformations, however, account for a significant fraction of observed events. For neutral lipids (C-D), PC lipids and PC/PE mixtures at high salt concentrations favor distal conformations (C), while (D) PE lipids, PC/PE mixtures at low salt concentrations, and DPhPC lipids favor proximal conformations. Created with [Biorender.com](https://www.biorender.com).

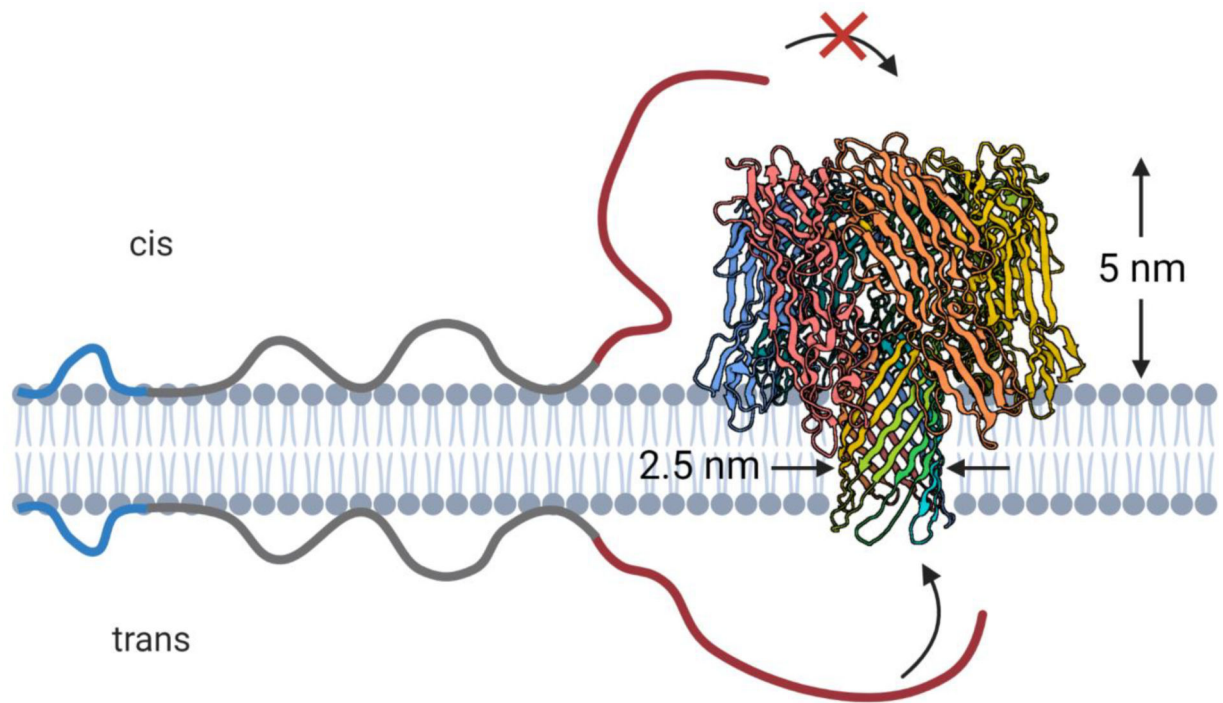


Figure 9.

The asymmetric structure of α -hemolysin (PDB ID: 3ANZ) prevents capture of membrane-bound α Syn from the cap (*cis*) side but allows capture from the stem side. Created with [Biorender.com](https://www.biorender.com).

Table 1.

Summary of results of VDAC nanopore-based analysis of α Syn-lipid interactions. Except for DPhPC, all lipids contained dioleoyl acyl chains.

<i>Lipid composition</i>	2PG/PC/PE		DPhPC^a	PE	PC/PE		PC	2TAP/PC/PE	
<i>Ionic strength (mM)</i>	150	1000	1000	1000	150	1000	1000	150	1000
<i>K_{off}(nM⁻¹s⁻¹) (-35 mV)</i>	108	38	29	33	99	8.9	4.3	5.65	1.4
Fraction $\tau_{off}^{(2)}$ (%)	< 10	< 10	<10	< 10	< 10	32	36	14	37
<i>x_b (nm) for $\tau_{off}^{(1)}$</i>	15.4	14.5	12.9	10.1	13.9	10.7	11.6	6.2	7.2
<i>x_b (nm) for $\tau_{off}^{(2)}$</i>	---	---		---	---	>17.2	>18.7	<i>b</i>	<i>b</i>
<i>E_b/k_BT for $\tau_{off}^{(1)}$</i>	35.7	19.0	18.3	15.0	29.3	15.0	15.8	18.4	14.8
<i>k_d (μM)^b</i>	47	---	---	---	1500	---	---	116	---

^aUsing data from [101].

^bThese were not characterized because of the broad t_{off} distributions without clear separation between populations.

^cAs determined using FCS in [92].